TECHNISCHE HOCHSCHULE FRIDERICIANA
KARLSRUHE
AERODYNAMISCHES INSTITUT

AERODYNAMISCHES INSTITUT
TECHNISCHE HOCHSCHULE
KARLSRUHE, GERMANY

CONTRACT AF 61 (052)-861 20 May 1968

FINAL SCIENTIFIC REPORT

INVESTIGATIONS ON THE NONELASTIC BEHAVIOR OF THE UPPER MANTLE

1 May 1965 - 30 April 1968

Contract AF 61 (052)-861

STEPHAN MUELLER

Geophysical Institute
Technical University
Karlsruhe , Germany

This research has been sponsored by the
AIR FORCE OFFICE OF SCIENTIFIC RESEARCH
under Contract AF 61(052)-861 through the
European Office of Aerospace Research,
OAR, USAF, as part of the
Advanced Research Projects Agency's Project
V E L A - U N I F O R M

FINAL SCIENTIFIC REPORT

INVESTIGATIONS ON THE NONELASTIC BEHAVIOR OF THE UPPER MANTLE

1 May 1965 - 30 April 1968

STEPHAN MUELLER
Principal Investigator

with contributions by

J. ANSORGE
K. FUCHS
D. MAYER-ROSA
D. SEIDL
U. WALTER
G. WOLBER

---

a)	ARPA Number:	612 - 1
b)	Name of Contractor:	Technical University of Karlsruhe Geophysical Institute Karlsruhe, Germany
c)	Dollar Amount of the Contract:	$ 81,000.00
d)	Date of the Contract:	5 April 1965
e)	Contract Number:	AF 61 (052) - 861
f)	Duration of the Contract:	1 May 1965 - 30 April 1968
g)	Project Scientist:	Mr. William J. Best
h)	Title of the Project:	VELA - UNIFORM
i)	ARPA Code (5810) Project:	9714

A B S T R A C T

The attenuation of seismic waves in the crust and upper mantle has been studied by various techniques in order to determine the specific quality factor Q. Anelastic deficiencies of the propagation medium can only be separated after corrections are made for the effects of instrumental distortion, of the "receiver crust" and the "source crust", the lossless propagation through the mantle and the source mechanism.

Seismic refraction data have been compiled for a number of "source" and "receiver" regions in Europe. A refined velocity-depth distribution with two velocity reversals and an average value of $Q_p \approx 670$ have been obtained for the crust of the Bohemian Massif in Central Europe. The Q_p of the uppermost mantle was found to be about 250. Crustal transfer functions were calculated to test models of crustal structure derived by other methods. The radiation patterns for two types of explosive sources have been determined. Their shape is strongly affected by the source mechanism and crustal structure.

A new velocity-depth structure of the upper mantle in Europe has been derived from travel-time observations of large

explosions and earthquakes. At least three velocity reversals have been found down to depths of about 220 km. They correlate well with the distribution of earthquake focal depths. Surface-wave dispersion measurements are also in agreement with these new findings. Amplitude decay data for surface waves indicate that zones of low Q_S must exist at depths where the low-velocity channels were found.

Finally an average value of $\overline{Q_P} \approx 220$ for the deeper mantle has been obtained based on observations of two intermediate focus earthquakes. A comparison with corresponding $\overline{Q_S}$ data shows that $Q_P \approx Q_S$, i.e. that losses in pure compression cannot be neglected. Alternatively it is suggested that Q may be frequency-dependent, at least over an extended frequency band.

C O N T E N T S

		Page
1.	INTRODUCTION	1
	1.1 Previous Results	1
	1.2 Wave Propagation through the Crust-Mantle System	4
2.	THE RECEIVER SYSTEM	6
	2.1 The "Receiver Crust"	6
	2.2 Travel Times of P Waves and the Velocity Structure of the Crust	8
	2.3 Amplitude Decay and the Q_p Structure of the Crust	10
	2.4 Crustal Transfer Functions	14
3.	THE SOURCE SYSTEM	18
	3.1 The "Source Crust"	18
	3.2 Source Mechanisms	20
4.	STRUCTURE OF THE UPPER MANTLE IN EUROPE	24
	4.1 Propagation of Seismic Body Waves	24
	4.11 Travel Times from Large Explosions	24
	4.12 Travel Times and Amplitude Spectra from Earthquakes	31
	4.2 Dispersion of Seismic Surface Waves	40
	4.3 Amplitude Attenuation of Surface Waves	51
5.	ANELASTIC PROPERTIES OF THE DEEPER MANTLE	59
	5.1 Average Q of Compressional Waves ($\overline{Q_p}$)	59
	5.2 Implications on Loss Mechanisms	63
6.	REFERENCES	66
7.	CHRONOLOGICAL BIBLIOGRAPHY	70

1. INTRODUCTION

1.1 Previous Results

Attenuation of seismic waves has been measured for many years. But it is only recently that sufficient precision in observation has been achieved and that analytical techniques have been developed which make possible the inversion of the experimental body and surface wave data (ref. KNOPOFF, 1964; ANDERSON and KOVACH, 1964; ANDERSON and ARCHAMBEAU, 1964; BEN-MENAHEM, SMITH and TENG, 1965). The resultant distribution of attenuation versus depth for compressional and shear waves, usually described by the dimensionless quality factors Q_p and Q_s, is an important and valuable source of additional information with regard to the pressure, temperature, state and composition in the earth's interior. It supplements the velocity data and provides a measure of anelasticity, i.e. it permits a description of the deviation from perfectly elastic wave propagation.

Results of seismological investigations over the past decade have demonstrated beyond doubt that the structure of the earth's crust and upper mantle is much more complex than has been assumed until recently. It is no longer permissible to approximate the uppermost 300 to 400 km of the earth by a model consisting of a few isotropic, homogeneous, lossless flat layers, as is for instance still done in the interpretation of a number of geophysical data.

Phase velocity measurements of seismic surface waves have shown that beneath a highly differentiated crust a zone of low shear-velocity (V_S) must exist in the upper mantle at depths between 100 and 200 km (see Fig. 1, right). This zone which is associated with temperatures approaching the melting point of the material, probably has a higher electrical conductivity than the regions above and below it. Its upper boundary which in the Alps and in their northern foreland is found at a depth of about 80 km (ref. KNOPOFF, MUELLER and PILANT, 1966; SCHNEIDER, MUELLER and KNOPOFF, 1966) must be identical with the discontinuity which supposedly separates the resistosphere from the conductosphere. The seismic velocities in this asthenosphere channel which extends to a depth of about 200 to 220 km are lowered by about ten per cent. It will be shown subsequently that this simple picture is much too crude and requires considerable modifications.

In addition to these observations evidence has been presented that a distinct reversal of compressional velocity (V_P) must occur at depths between about 7 and 12 km within the continental crust (see Fig. 1, left). The interpretation of strong second arrivals on seismic refraction profiles as well as of large normal-incidence reflections requires the presence of a well-developed low-velocity zone in the sialic part of the crust overlying a layer whose velocity is markedly greater than the velocity in the channel and at least 0.2 km/sec higher than that above the channel (ref. MUELLER and LANDISMAN, 1966).

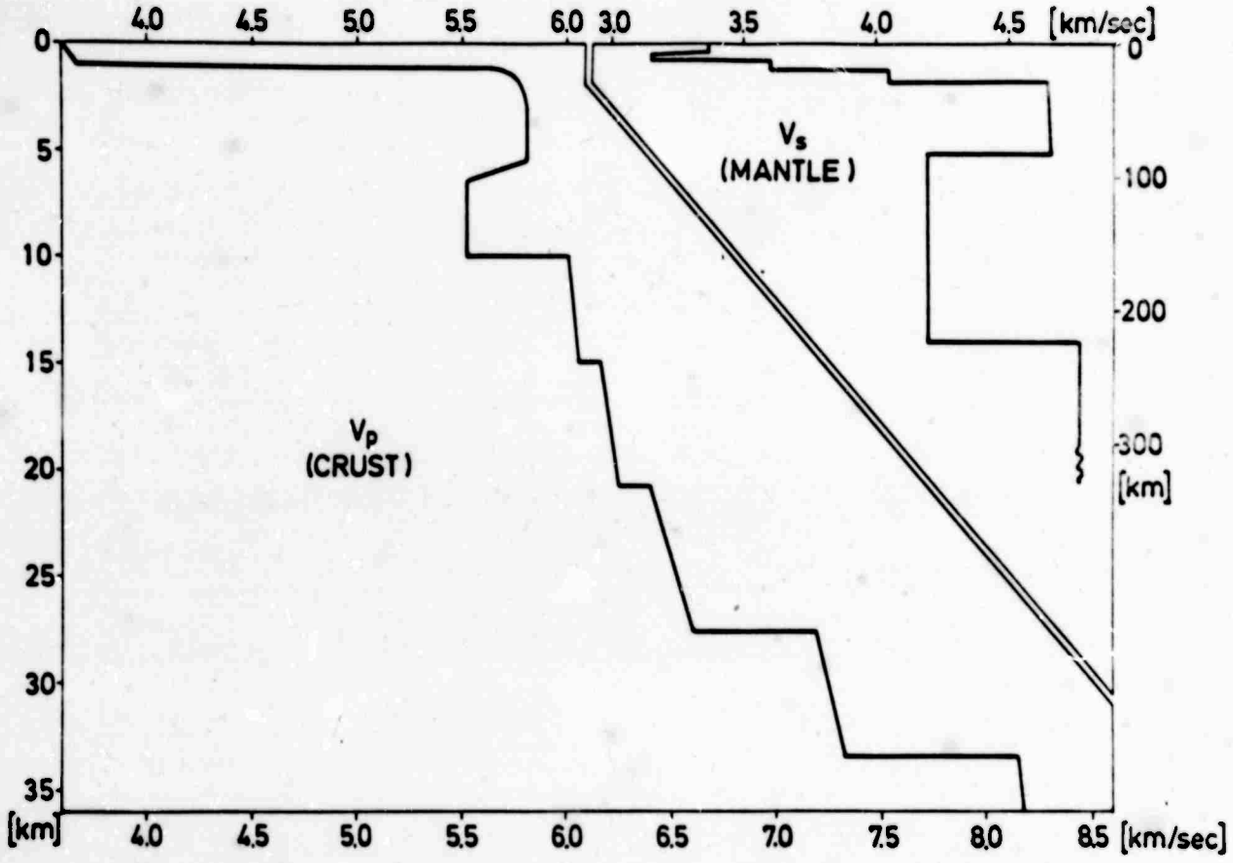

Fig. 1: Summary of velocity-depth distributions in the crust (V_p) and upper mantle (V_s)

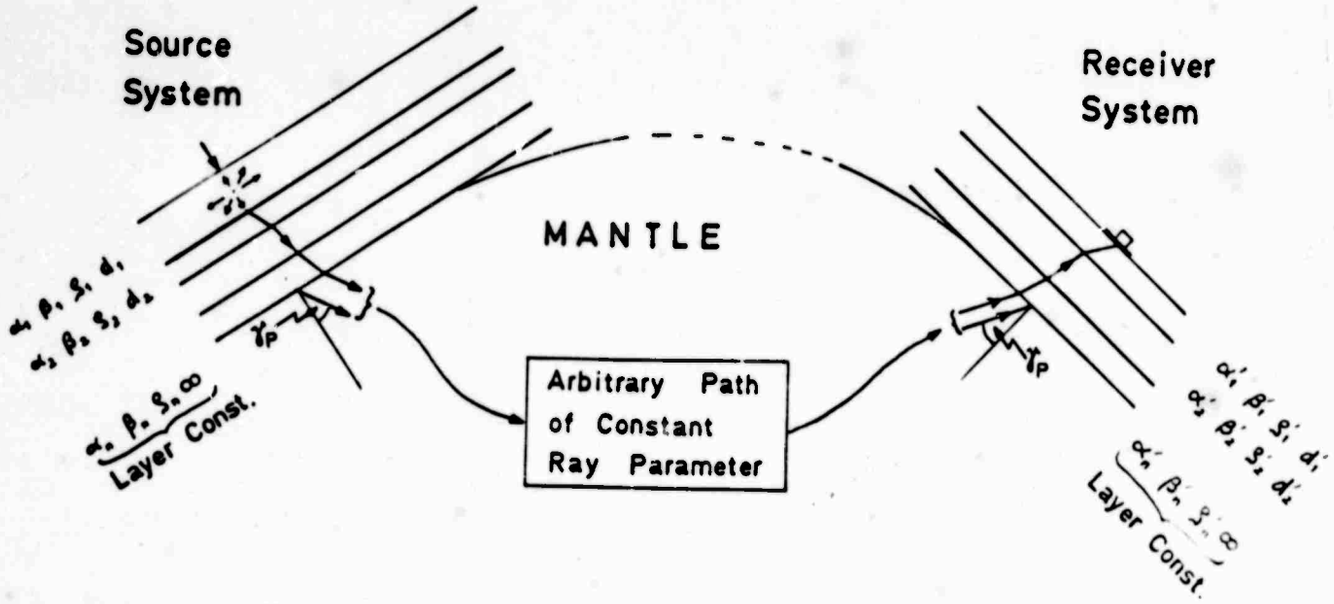

Fig. 2: Schematic diagram of wave propagation through the crust-mantle system

Furthermore it had been found necessary to divide the lower crust into several gradient layers in order to account for the more important arrivals seen on the seismograms. From a comparison of seismic refraction and reflection data in Central Europe it was concluded that the next two interfaces just below the sialic low-velocity zone seem to be associated with the so-called "Conrad discontinuity" in the northern and southern parts of Germany, respectively.

Some observations provide strong support to the proposed existence of an intermediate crustal layer just above the "Mohorovičić discontinuity" with velocities of about 7.5 km/sec (ref. LANDISMAN and MUELLER, 1966; FUCHS and LANDISMAN, 1966 a+b). This high-velocity layer has been found now in many parts of Europe. Its average thickness must be of the order of 10 km. A typical case will be presented later on which emphasizes the necessity of introducing a second velocity reversal right on top of this high-speed layer.

1.2 Wave Propagation through the Crust-Mantle System

If the validity of a linear theory of wave propagation along a ray path from the source through the crust and mantle to the receiving station is assumed, the wave forms of the P and S signals at large enough distances are shaped by a number of factors which depend on the history of the signal as indicated in Fig. 2 According to this schematic diagram it should be possible to trace

back the signal character of a certain phase in the seismogram at the receiving station through the recording instrument, the receiver system, the "homogeneous mantle" and the source system to the source.

In a realistic model of the earth the complex structure of the crust and upper mantle both at the source and the receiver location must be taken into account. To a first approximation the inhomogeneous crust and uppermost part of the mantle are replaced by a system of (n-1) homogeneous isotropic layers with plane parallel interfaces as shown in Fig. 2 (ref. FUCHS, 1966). The compressional velocity, the shear velocity, the density and the layer thickness of the $i^{\underline{th}}$ layer have been denoted by α_i ($= V_{pi}$), β_i ($= V_{Si}$), ρ_i, and d_i, respectively. Primed symbols refer to the "receiver system", while unprimed quantities describe the "source system". The top layer (index 1) in either of the two systems is specified to have a free surface.

The $n^{\underline{th}}$ layer representing the deeper mantle is assumed to be relatively homogeneous, i.e. the elastic properties in this "half space" vary more gradually than they do in the differentiated system of the crust and upper mantle. In Fig. 2 the angle γ_p is the angle of incidence for P waves at the base of the receiver system which for a particular ray is equal to the angle of radiation into the mantle at the base of the source system.

A vertical point force acting on the free surface of the source system has been used as the simplest model of an atmospheric explosion. For underground

explosions an impulsive source situated at a shallow depth h in the top layer has been assumed. If the dimensions of the source region are small compared to the distance from the layer boundaries, the source may be regarded as a concentrated point source.

2. THE RECEIVER SYSTEM

Before the distorting effects of the earth's crust and upper mantle on the spectrum of seismic signals are discussed, it should be emphasized that all signal phases recorded on a seismogram have to be corrected for the amplitude and phase response of the recording instrument. In the subsequent analysis proper care is taken of this instrumental correction except for cases where it is specifically mentioned.

2.1 The "Receiver Crust"

The comparatively inhomogeneous structure of the crust and upper mantle gives rise to considerable signal distortion as has been pointed out before. The spectral behavior of the receiver system must therefore be known quite accurately, and this in turn requires a detailed knowledge of crustal and upper mantle structure in the European area. A comprehensive survey of crustal investigations in Central Europe has been undertaken in order to provide the required information.

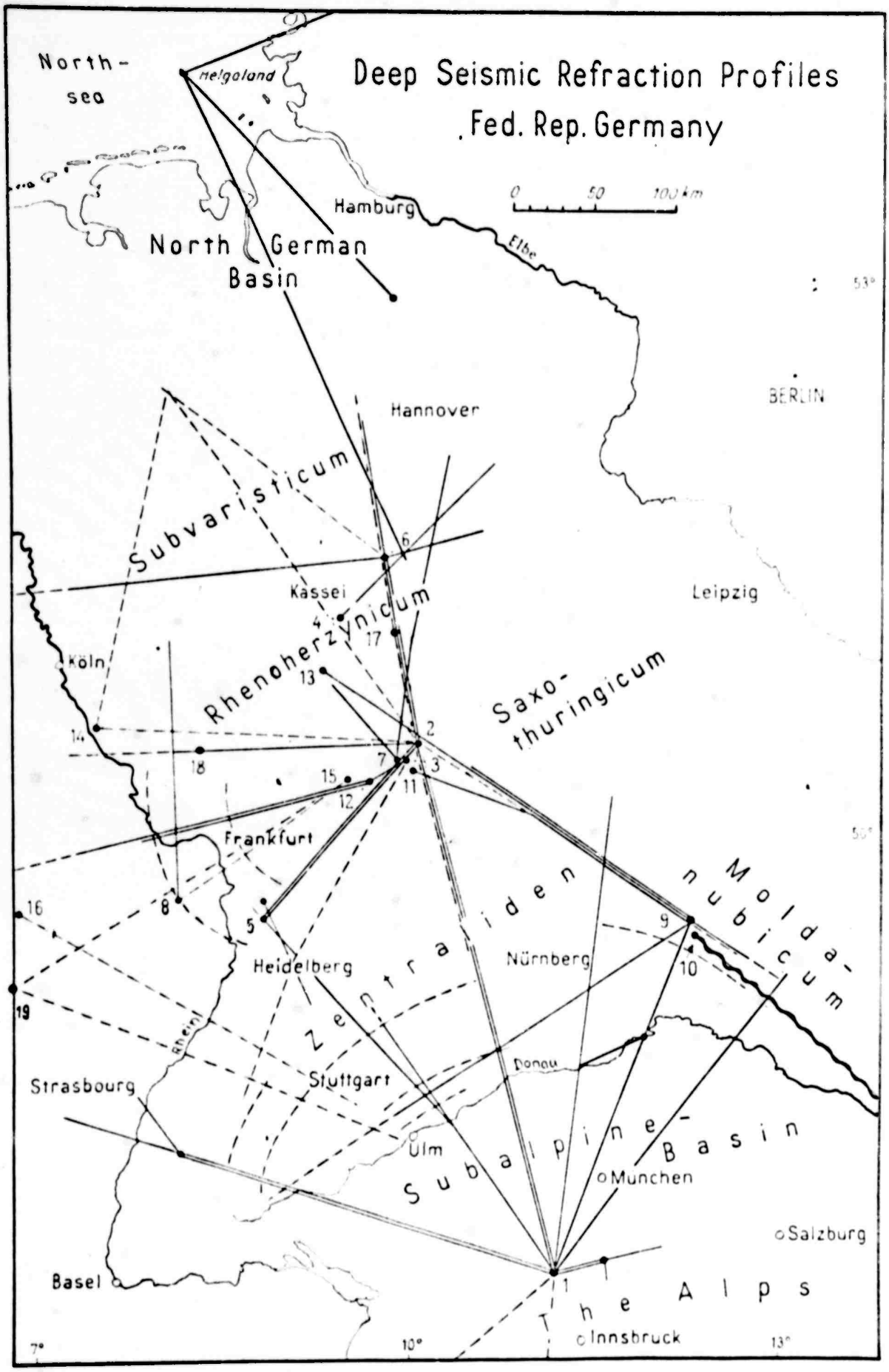

Fig. 3: Map of seismic refraction profiles in Central Europe (after A. STEIN)

In Fig. 3 all seismic refraction profiles are compiled which have been studied since 1947. For about ten years all geophysical institutes, state geological surveys and geophysical prospecting companies in the Federal Republic of Germany cooperate closely within an extensive research program called the "Determination of Crustal Structure in Central Europe". This program is sponsored by the German Research Association (Deutsche Forschungsgemeinschaft).

Wherever possible observations were carried out in reverse directions and along overlapping profiles. These are marked in Fig. 3 by double lines and broken lines, respectively. The shotpoints are denoted by black dots at the end of each line and are numbered consecutively. A preliminary interpretation of most of these measurements has been published some years ago by the GERMAN RESEARCH GROUP FOR EXPLOSION SEISMOLOGY (1964).

2.2 Travel Times of P Waves and the Velocity Structure of the Crust

(G.WOLBER)

An example for a presumably homogeneous path of propagation is provided by a line running southeastward from shotpoint 10 (VOGGENDORF) in Fig. 3 parallel to the margin of the Bohemian Massif. This profile starts about 90 km east of the Gräfenberg Seismological Observatory in the "Moldanubicum". It is 240 km long and extends far into Austria. A total of 52 stations with identical instruments were occupied, all located on crystalline outcrops of the Bohemian Massif.

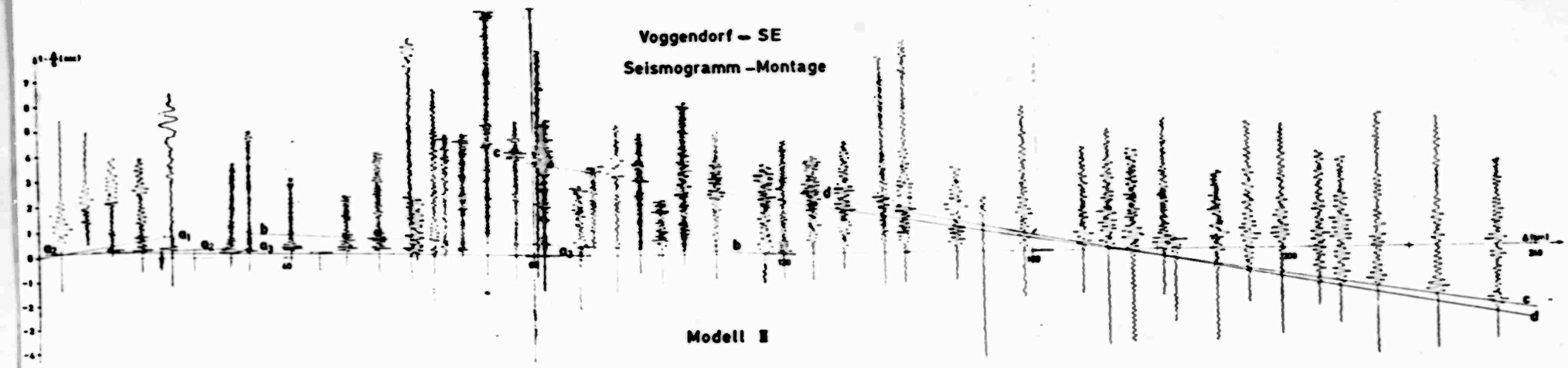

Fig. 4: Record section for the VOGGENDORF-SE profile with signal correlations

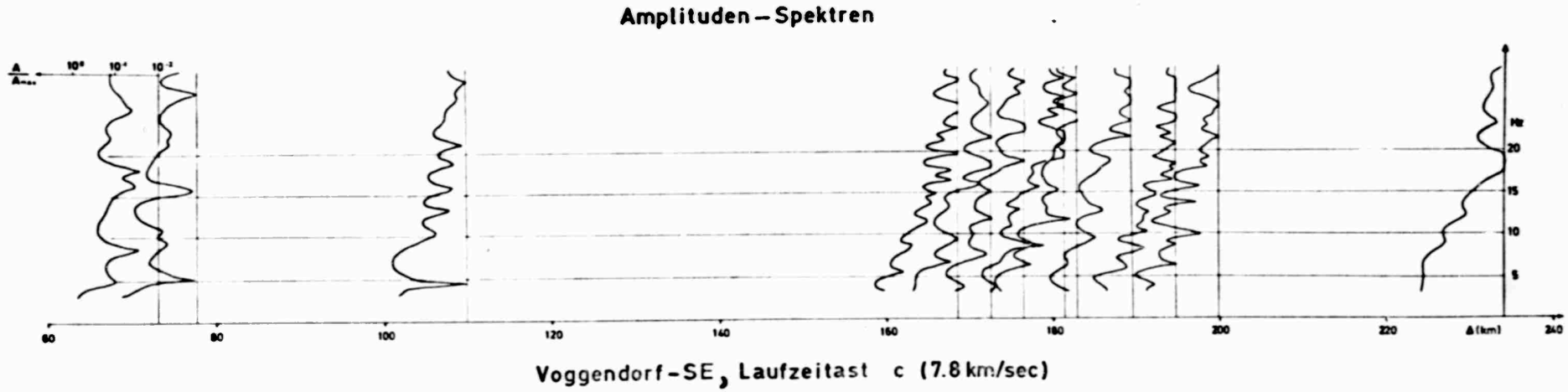

Fig. 5: Amplitude spectra for travel-time branch c (7.8 km/sec) of the VOGGENDORF-SE profile

In Fig. 4 a seismogram section with correlations is shown for this profile VOGGENDORF - SE. All records were digitized manually and then brought to the same reduced time scale by a digital plotter. Four major travel-time branches (a, b, c, d) could be identified. A velocity-depth structure V_p (z) has been determined from the correlations drawn.

The result is shown in Fig. 7 (left). Below a pseudo-gradient zone near the surface t w o velocity reversals had to be introduced in order to explain the overlapping travel-time curves b and c in Fig. 4 (ref. LANDISMAN, MUELLER and FUCHS, 1967). As mentioned earlier the existence of a high-speed layer with a P velocity of 7.8 km/sec just above the classical Mohorovičić discontinuity must be assumed if the duplication of the first arrivals at greater distances is to be explained. These new crustal features are presently explored in more detail.

2.3 Amplitude Decay and the Q_p Structure of the Crust

(C.WOLBER)

Following the schematic diagram in Fig. 2 the data processing starts with a spectral analysis of the observed seismogram which is then corrected for the effects of instrumental distortion. A schematic flow diagram of the harmonic analysis procedure is presented in Fig. 6. The computer program reads, checks, filters, decimates and windows the data before it performs the frequency analysis. Optionally the output is listed, plotted or punched on cards.

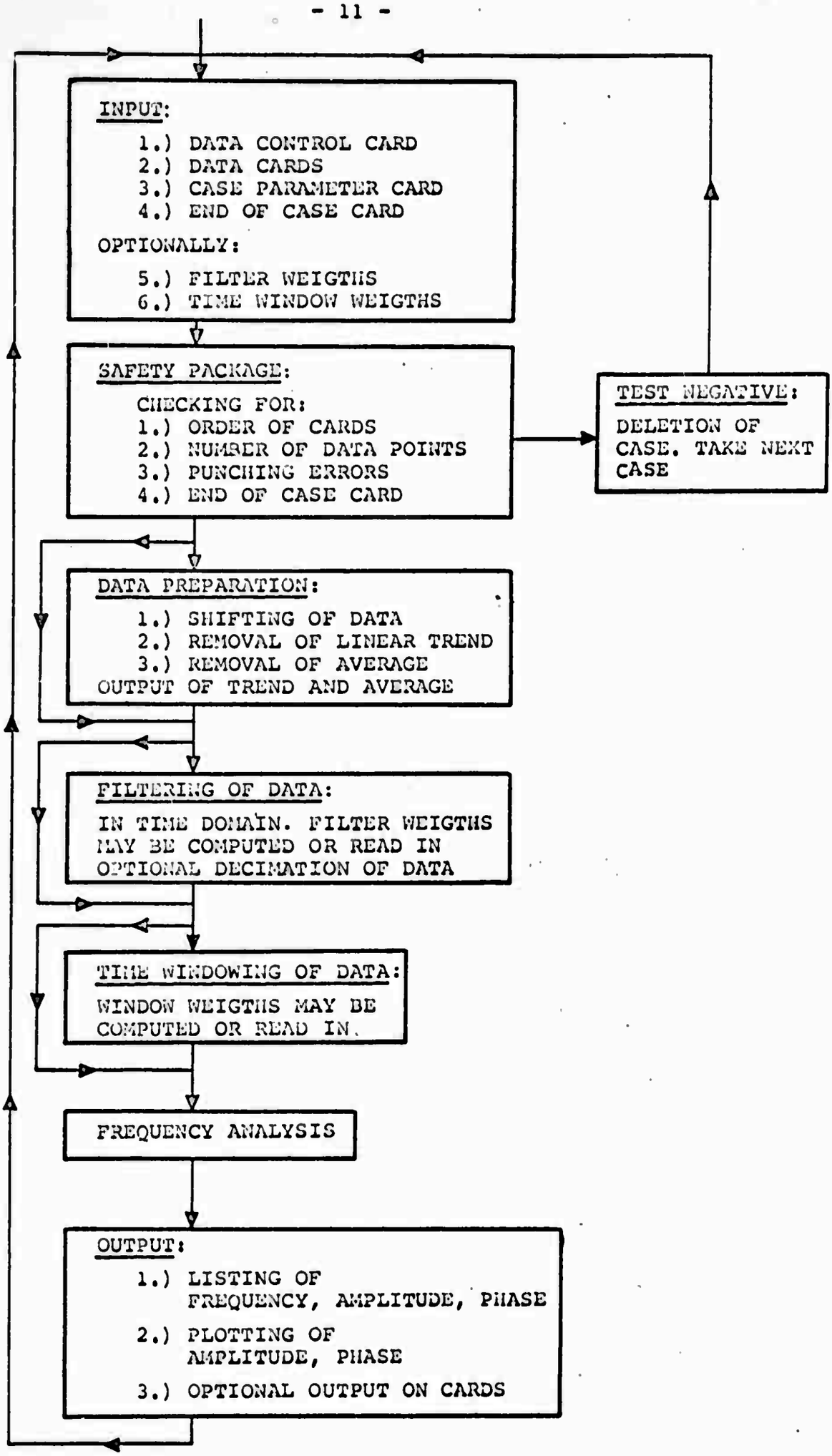

Fig. 6: Schematic flow diagram of spectral analysis program

Spectral analyses of the correlated seismogram phases in the record section of Fig. 4 have been used to deduce an average specific quality factor Q for P waves (Q_p) in the crust of the Bohemian Massif. If the amplitude response of the explosive source and of the receiver are known, any systematic variation of the observed signal spectrum must be due to variation in the spectral response of the propagation system. This response is determined by the geometry of the transmission path and by anelastic deficiencies of the propagation medium. For distances large compared with the depth of penetration the geometry should not have any influence on the amplitudes unless the medium is severely inhomogeneous in lateral directions. Under these simplifying assumptions any frequency-dependent amplitude decay may be attributed to absorption and - to a minor degree - to scattering.

In Fig. 5 the amplitude spectra are shown for the travel-time branch c (7.8 km/sec) as correlated in Fig. 4. All the spectra in our analysis have been corrected individually for instrumental distortion. Following a well-known procedure (see e.g. O'BRIEN, 1967) the spectral gradients were then determined for each spectrum in the distance range given. From a plot of spectral gradients versus range an average value for Q_p could be estimated provided a representative value for the P wave velocity (V_p) was chosen.

Assuming ideal head-wave propagation the velocity-depth distribution in Fig. 7 (left) could be used. With this model a least-squares solution led to a mean Q_p of 670 $\pm$ 100 for the upper

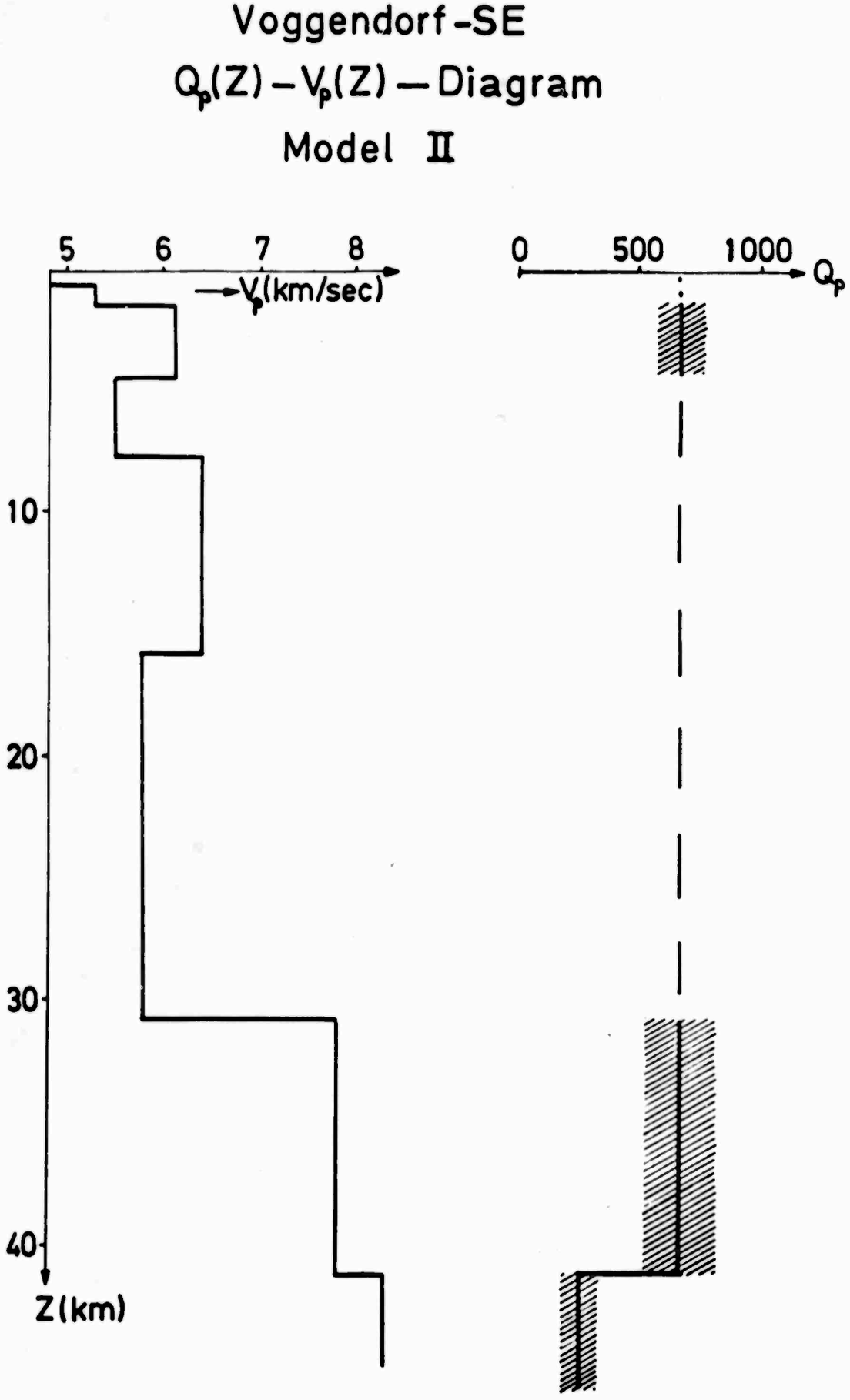

Fig. 7: V_p (z) and Q_p (z) distribution for the VOGGENDORF-SE profile

crust and of 670 $\pm$ 150 for the lower crust (see Fig. 7, right). For the uppermost mantle a Q_p of 250 $\pm$ 80 has been found. There are some indications that a gradual decrease of Q_p occurs in the transition region between crust and mantle. Determinations of Q_p for the middle crust gave values around 450 with a relatively high error. The Q_p structure presented in Fig. 7 (right) is far from being complete, but demonstrates that the Q_p values for the crust inferred from Q_S measurements (ref. PRESS, 1964; ANDERSON, BEN-MENAHEM and ARCHAMBEAU, 1965) seem to be too high by a factor of about two.

2.4 Crustal Transfer Functions

(K. FUCHS)

Since results of seismic refraction measurements are only available for a few areas in Europe a program has been initiated to check and supplement these data by determining the influence of the "receiver crust" on the spectral behavior of long-period body waves. Theoretical transfer functions for the crust-mantle system have been calculated following earlier investigations by PHINNEY (1964), HANNON (1964), FERNANDEZ (1967) and BEN-MENAHEM, SMITH and TENG (1965). A comparison of these theoretical transfer functions with experimental results have enabled us to test models of crustal structure in regions where the results of other methods, such as travel time studies and surface-wave dispersion measurements, did not lead to a consistent picture.

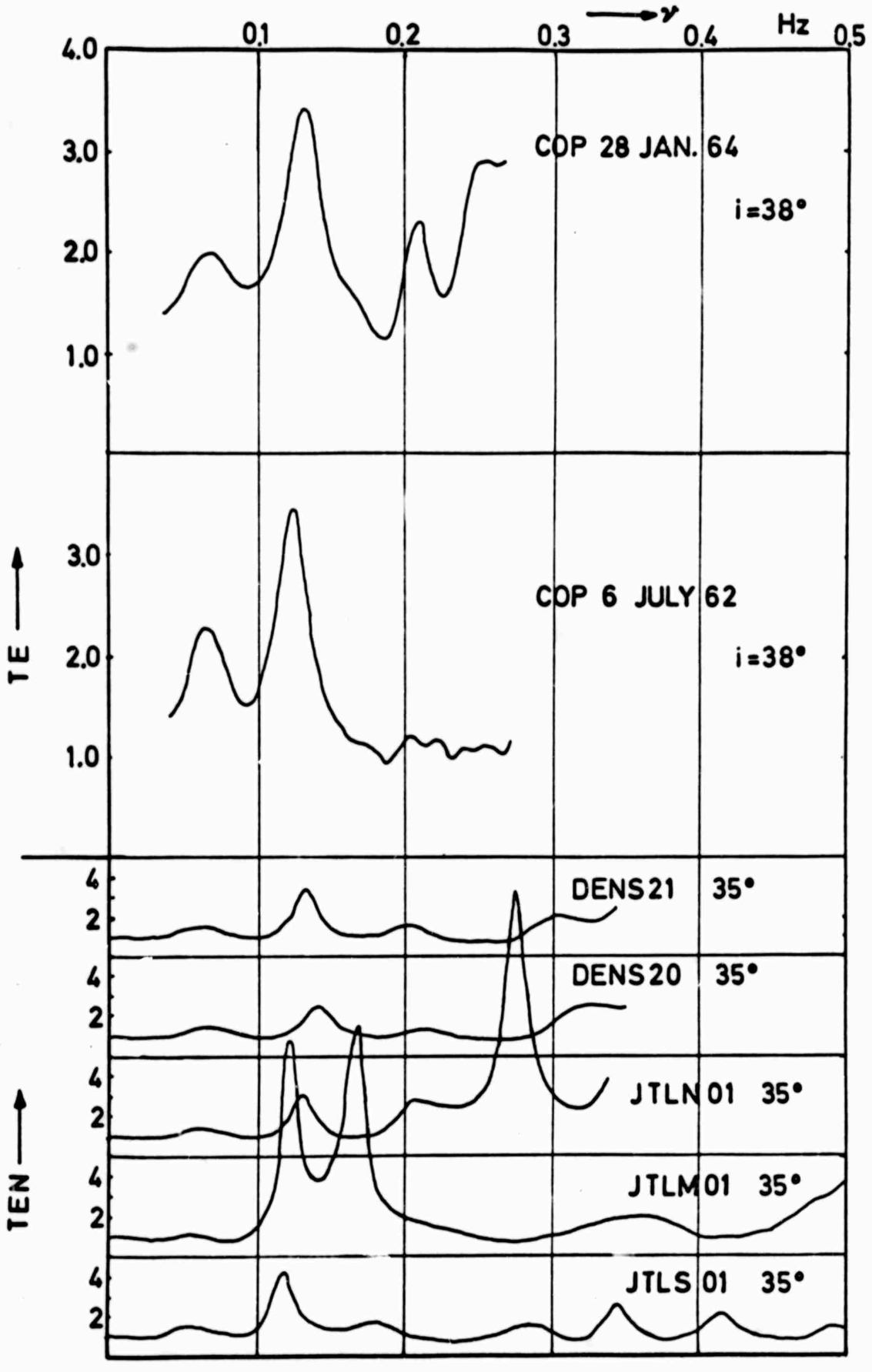

Fig. 8: Comparison of experimental and theoretical crustal transfer functions for Denmark (COP). i is the angle of incidence at the base of the crust.

Depth (km)	Thickness (km)	V_P (km/s)	V_S (km/s)	Density (g/cm^3)
	1.9	3.0	1.732	2.33
1.9	6.4	6.1	3.522	2.86
8.3	19.5	6.6	3.811	3.00
27.8		7.9	4.561	3.38
Model DENS 20 - Denmark (HIRSCHLEBER, HJELME, SELLEVOLL, 1966)				
	1.9	3.0	1.732	2.33
1.9	6.4	6.1	3.522	2.86
8.3	21.0	6.6	3.811	3.00
29.3		8.2	4.734	3.43
Model DENS 21 - Denmark (HIRSCHLEBER, HJELME, SELLEVOLL, 1966)				
	2.70	3.0	1.73	2.20
2.70	8.53	6.0	3.46	2.75
11.23	18.17	6.7	3.87	2.95
29.40		8.1	4.67	3.40
Model JTLN 01 - Denmark (HIRSCHLEBER, 1964; pers. communication)				
	5.10	3.0	1.73	2.20
5.10	6.67	6.0	3.46	2.75
11.77	18.23	6.7	3.87	2.95
30.00		8.1	4.67	3.40
Model JTLM 01 - Denmark (HIRSCHLEBER, 1964; pers. communication)				
	1.05	3.0	1.73	2.20
1.05	11.15	6.0	3.46	2.75
12.20	20.60	6.7	3.87	2.95
32.80		8.1	4.67	3.40
Model JTLS 01 - Denmark (HIRSCHLEBER, 1964; pers. communication)				

Table 1: Crustal Models in Denmark

Depth (km)	Thickness (km)	V_p (km/s)	V_S (km/s)	Density (g/cm^3)
	4.75	3.98	2.38	2.34
4.75	17.00	5.90	3.30	2.82
21.75	11.25	6.58	3.80	2.92
33.00		8.14	4.70	3.30
Model IB 1 - Iberian Peninsula (PAYO, 1965)				
	4.7	3.94	2.37	2.34
4.7	18.3	5.90	3.30	2.80
23.0	10.0	6.60	3.70	2.85
33.0		8.10	4.72	3.30
Model IB 2 - Iberian Peninsula (PAYO, 1965)				

Table 2: Crustal Models of the Iberian Peninsula

As an example the spectral ratio TE (ν) of the vertical component W (ν) to the horizontal component U (ν) is shown in Fig. 8 for two deep-focus earthquakes as recorded at Copenhagen (COP), Denmark. The theoretical transfer functions TEN (ν) for various crustal models of Denmark are compared with the experimental results. It is seen that the crustal models DENS 20 and JTLN 01 (see Table 1) come closest to the observations with regard to peak ratio and frequency.

A similar analysis has been carried out for station Toledo (TOL), Spain. It could be shown that the crustal model IB 2 (see Table 2) of PAYO (1965) provided a much better fit to the data than model IB 1 (ref. Table 2) which we had used in our previous investigations (MUELLER and FUCHS, 1966).

3. THE SOURCE SYSTEM

(K. FUCHS)

3.1 The "Source Crust"

Since no direct determinations of crustal structure are available for the source areas covered in our studies the elastic properties of the earth's crust in those regions had to be inferred by extrapolation of published results. For Novaya Zemlya and the Barents Sea the two crustal models NUR-1 (PENTTILÄ, 1965) and URAL (DEMENITSKAYA, 1961) depicted in Fig. 9 were chosen to give an estimate of the crustal structure under Novaya Zemlya.

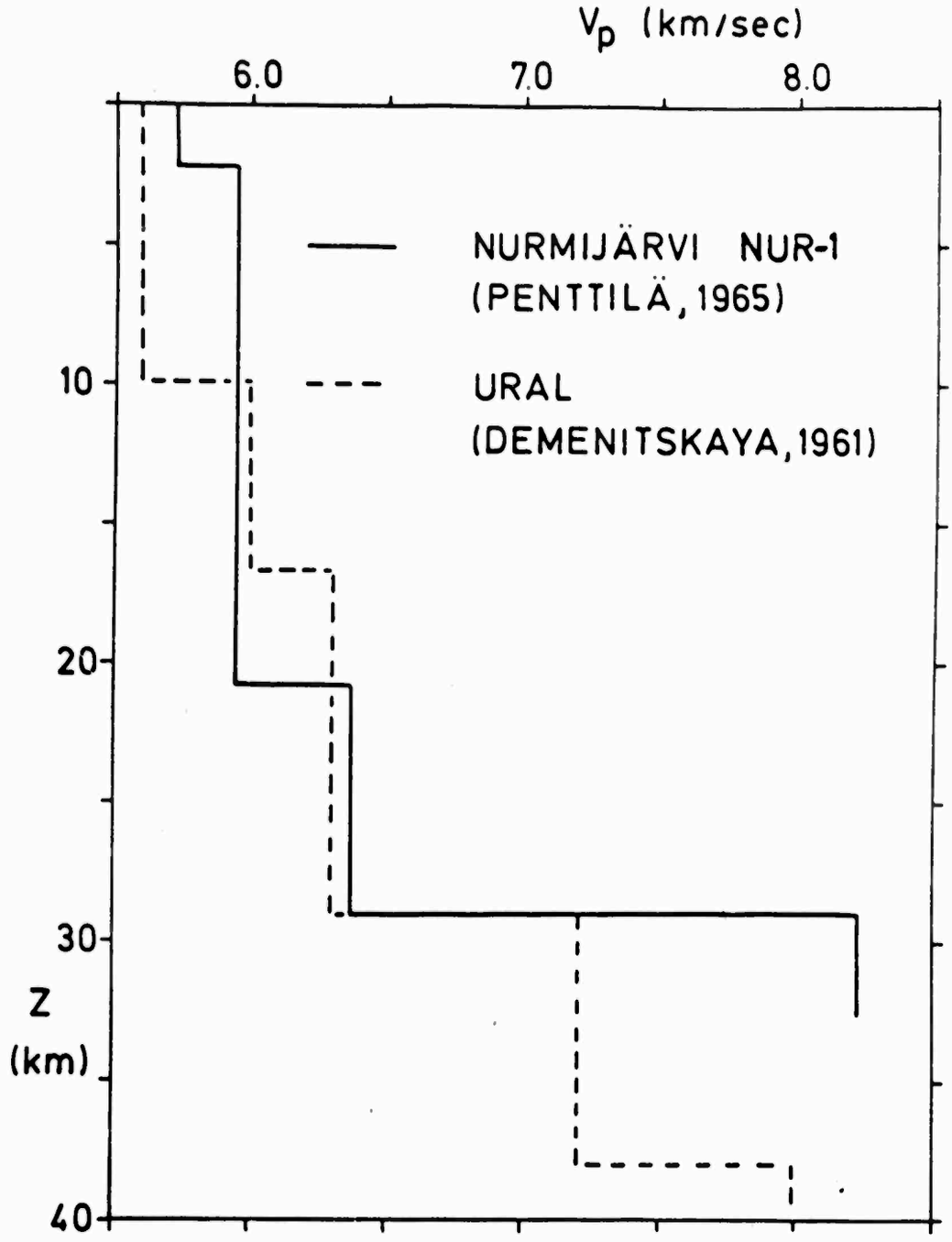

Fig. 9: "Source crust" models NUR-1 and URAL

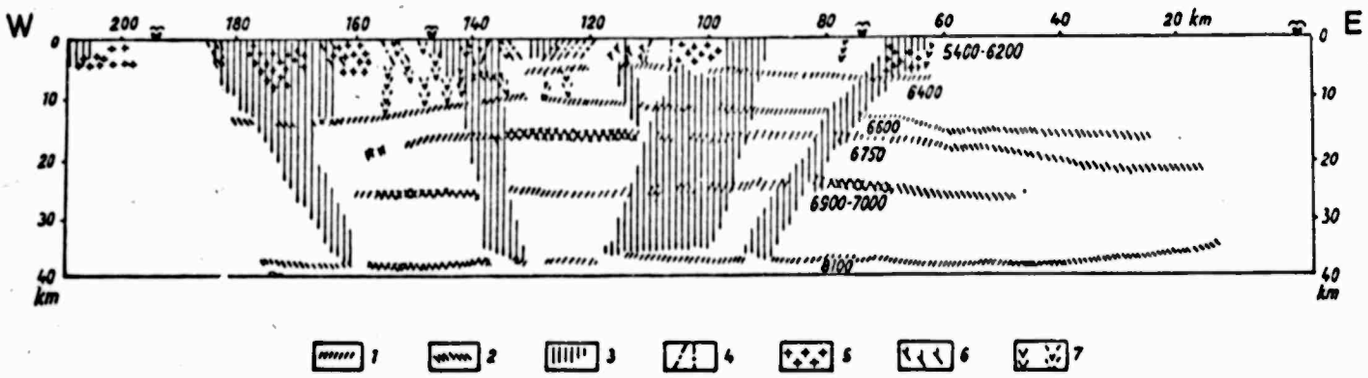

Fig. 10: Crustal section for the profile UCHTA-KEM in Karelia (U.S.S.R.) - Explanation of legend see text

A better approximation is probably given by the crustal section of LITVINENKO and NEKRASOVA (1962) for the profile UCHTA-KEM in Karelia reproduced in Fig. 10. The symbols used in the section are explained as follows:

1 = Interface found from head waves
2 = Interface found from reflected waves
3 = Fault zone determined by deep seismic sounding
4 = Fault zone determined by field geology
5 = Granite bodies
6 = Granodiorite zones
7 = Regions with basic and ultrabasic rocks

The values of P velocity are given in meters per second. It is seen that the main features of this crustal model are similar to the ones of our preferred model URAL. Both structures are presently investigated if they do provide a satisfactory explanation for the spectral behavior of long-period body waves recorded at nearby observatories in Finland.

3.2 Source Mechanisms

A vertical point force acting on the free surface of a layered system (see Fig. 2) has been used in an attempt to evaluate the influence of the earth's crust and the uppermost mantle on the spectrum of seismic body waves excited by atmospheric explosions. The radiation pattern for the far field has been calculated at a number of discrete frequencies for the two crustal models NUR-1 and URAL (see Fig. 9). Fig. 11 demonstrates how differences in crustal structure of the source region affect the shape of the radiation pattern.

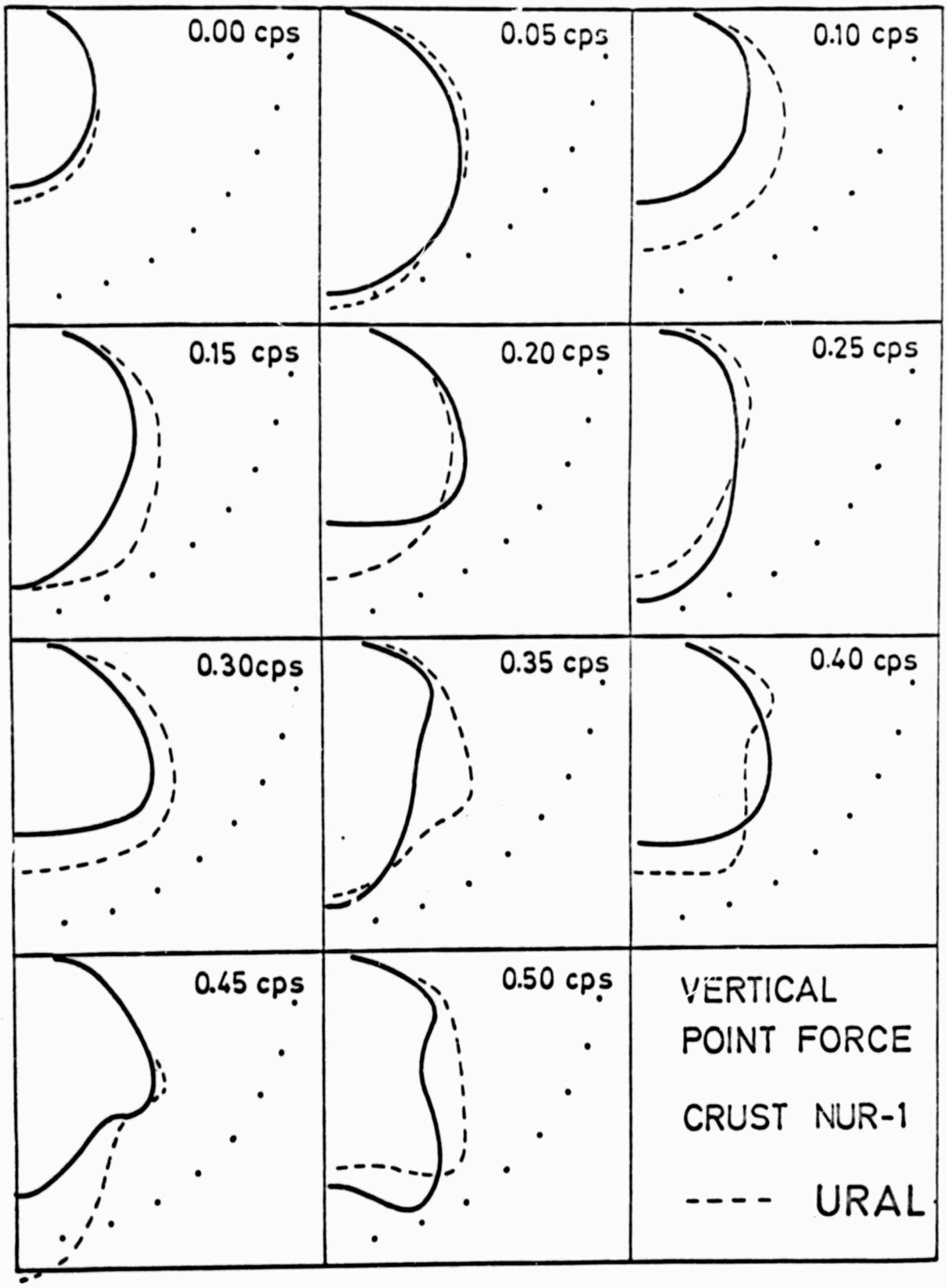

Fig. 11: Radiation pattern for a vertical point source acting on the free surface

For underground explosions an impulsive point source buried at some depth within the crust served as an adequate model. The transfer function for this configuration has been derived by FUCHS (1966). In Fig. 12 the radiation patterns in the frequency range from 0 to 0.5 cps are shown for the two "source crust" models. As before only the right half of the symmetrical pattern has been drawn. A clear directional effect is seen.

The radiation pattern of the buried explosive source differs significantly from that of the vertical point force. In the case of the buried source a strong primary reflection is generated at the free surface of the crust. Its interference with the primary wave strongly shapes the radiation pattern. The surface reflection is, of course, absent in the case of the point force acting on the free surface. Experimentally determined amplitude-distance curves will be influenced by the frequency-dependent distortions of the radiation pattern. This effect is presently being analyzed more thoroughly.

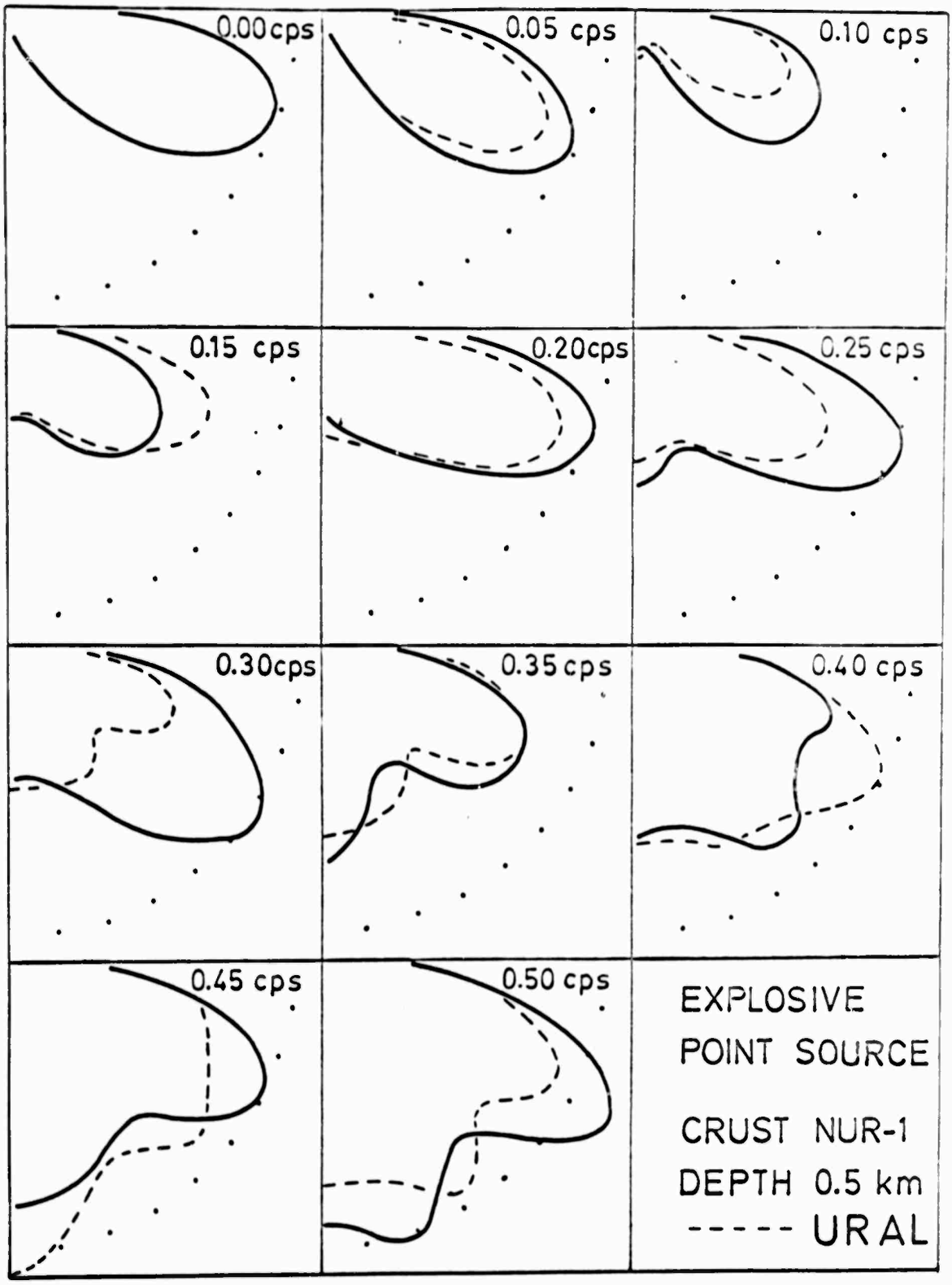

Fig. 12: Radiation pattern for an explosive point source buried at a depth of 0.5 km

4. STRUCTURE OF THE UPPER MANTLE IN EUROPE

4.1 Propagation of Seismic Body Waves

4.11 Travel Times from Large Explosions

(J. ANSORGE)

Travel time studies of earthquake events suffer from the inherent inaccuracies of epicenter location and origin time. We have therefore tried to obtain more accurate travel time data in Europe for the distance range to 10° by using large explosions. A number of artificial events recorded along suitable long-range profiles were carefully analyzed in an attempt to resolve the apparent discrepancies between earthquake and explosion observations. In Fig. 13 long-range seismic refraction lines are shown for 4 selected events:

(1) The HELGOLAND Explosion of 18 April 1947
Charge size about 8000 tons of ammunition
Length of SSE profile: 640 km

(2) The LAC NEGRE Explosions of September 1966
Charge sizes up to 40 tons
Length of N profile: 700 km

(3) The LAC de l'EYCHAUDA Explosion of 22 September 1963 (BEAUFILS, MECHLER and ROCARD, 1965)
Charge size: 2 tons
These data could be combined with observations of (2) to provide an overlapping profile.
Length of NW profile: 800 km

(4) The FOLKSTONE Explosion of 22 July 1967
Charge size about 500 tons
(Magnitude M = 4.7 according to USCGS)

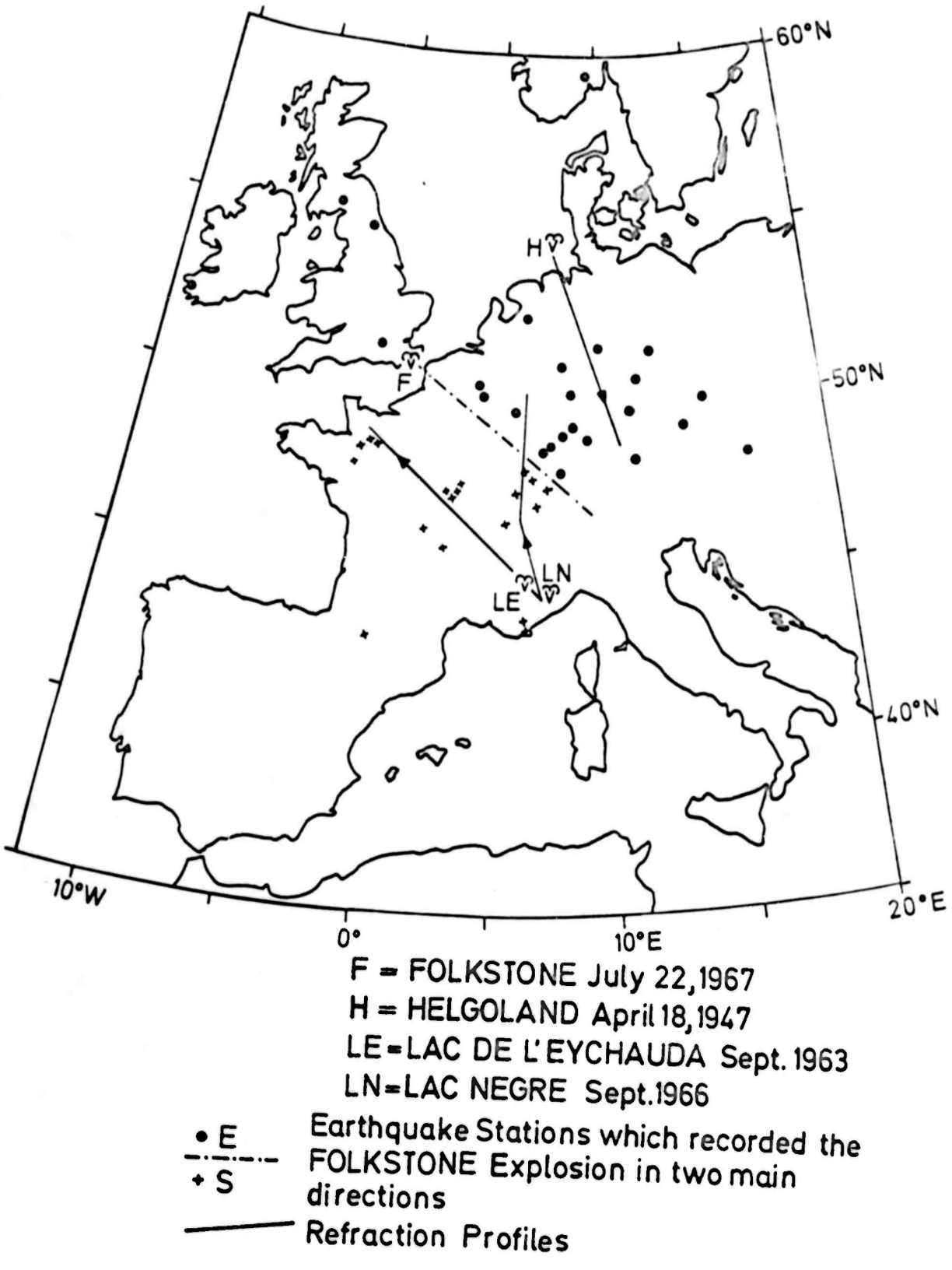

Fig. 13: Map of long-range seismic refraction profiles in Europe

(a) Observations in Central Europe to 10° - The earthquake stations in Central Europe were groped in two main azimuthal directions - a distinction which turned out to be unnecessary in this distance range

(b) Observations in Scandinavia to 20° - presently being analyzed.

All these long-range seismic measurements have shown that the distribution of compressional velocity (V_p) with depth in the uppermost part of the mantle is much more complicated than hitherto assumed. It also differs significantly from region to region. For a long time it has been suspected that a velocity inversion for P waves should accompany the shear-wave low-velocity channel found in the upper mantle at depths between about 100 and 200 km.

The timed explosions so far analyzed have consistently produced evidence for a triplication of the P wave travel time curve in the distance range between 4° and about 7°. With the high time resolution of our new field equipment a new phase could be identified which was termed P_m, (see Fig. 14). Typical values for the surface velocity of this phase lie between 8.25 and 8.35 km/sec, while for P_n ($= P_d$) relatively low values between 8.05 and 8.10 km/sec are measured. The new phase explains the previously observed break or jump in the first arrival curve around 9°.

In Fig. 15 the explosion data of the LN-LE NW profile (see Fig. 14) are plotted in conjunction with earthquake data for events of about the same epicentral location. If the latter are reduced to zero focal depth both sets of observations can be combined yielding a very

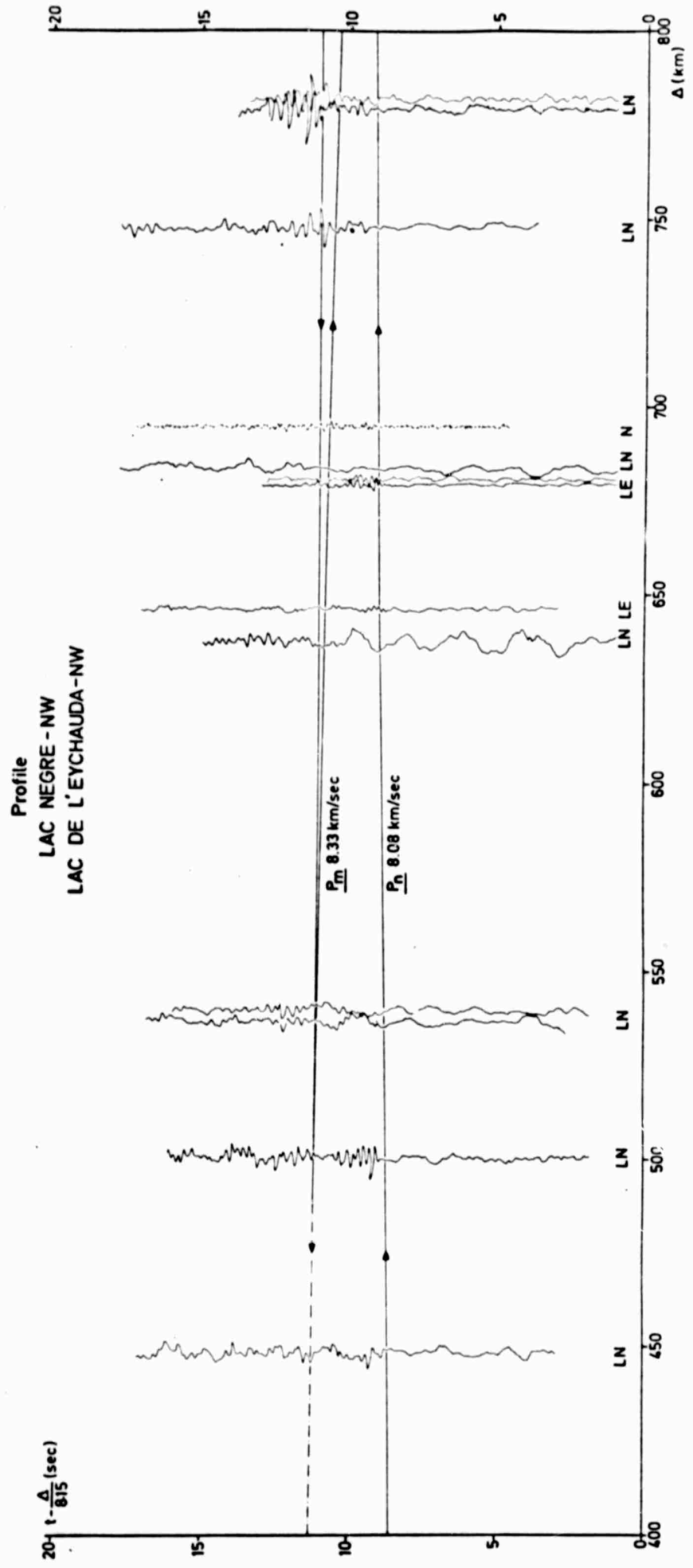

Fig. 14: Combined record section for the LAC NEGRE-NW and LAC DE L'EYCHAUDA-NW profiles

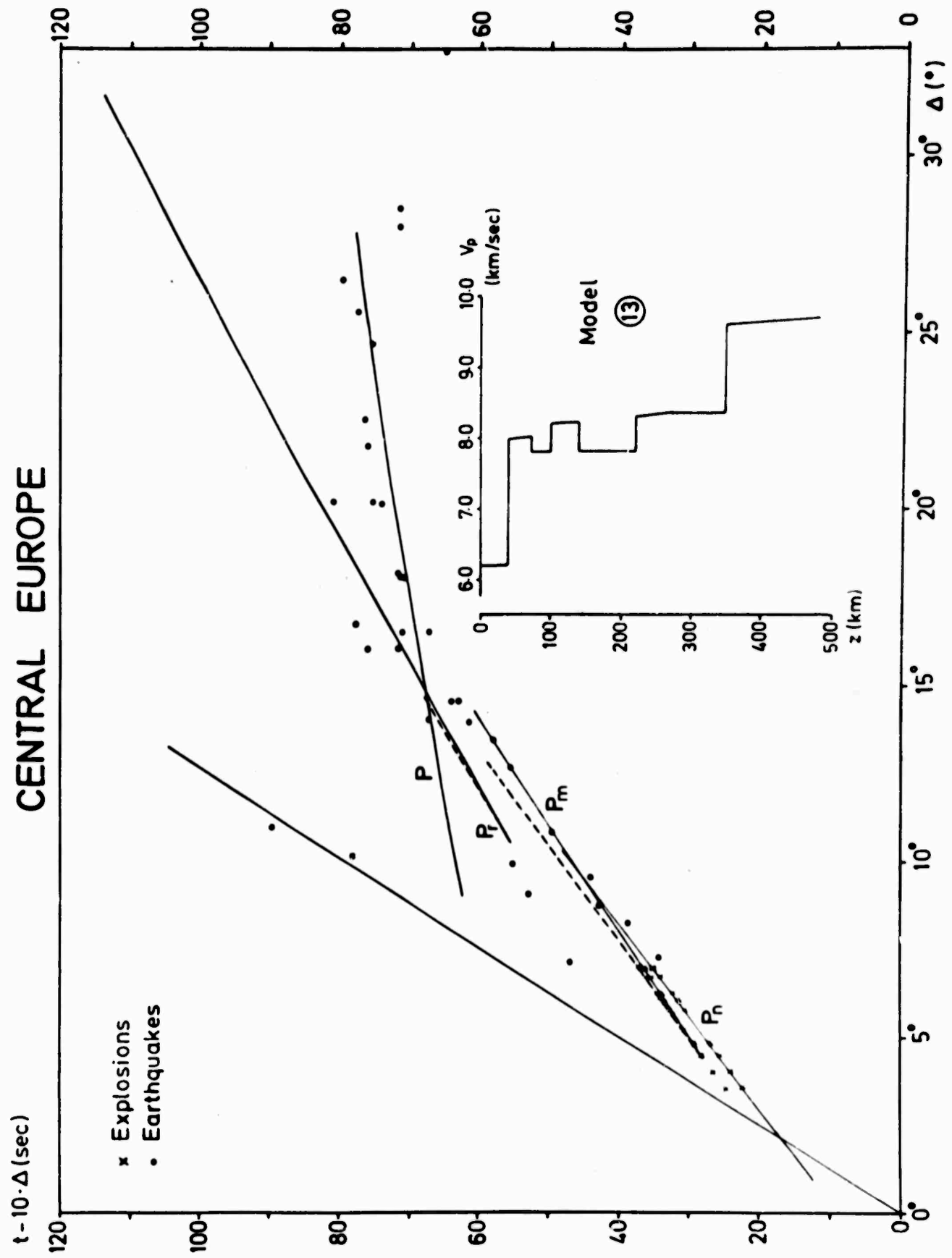

Fig. 15: Travel times from large explosions and earthquakes in Central Europe ($P_n = P_d$) with deduced velocity-depth model 13

consistent travel time pattern for Central Europe.

The velocity distribution for Model (13) depicted in Fig. 15 provides a satisfactory explanation of the data. Two velocity reversals at depths between 70 and 220 km are required in the model in order to account for the observed overlap of the various travel-time branches (ref. MUELLER, ANSORGE, MAYER-ROSA and FUCHS, 1968).

Additional information on the structure of the uppermost mantle in Central Europe was obtained from the recordings of the FOLKSTONE Explosion (22 July 1967). The location of this event is precisely known, but the origin time given by USCGS and BCIS differ by 1.3 seconds. This discrepancy could be resolved by comparing the P_n observations with recent seismic refraction measurements in the British Channel between Cornwall and the Bretagne. From the apparent velocity and intercept-time the USCGS determination was found to be correct.

In Fig. 16 all readable signal onsets are plotted as a function of distance. Three travel-time branches could be correlated which seemed to be independent of azimuth. The duplication of the first arrivals in the distance range between 4° and 5° led to the identification of a P_{m1} and a P_{m2} branch with velocities of 8.12 and 8.31 km/sec, respectively. At close-in distances a P_n velocity of 8.05 km/sec was measured. The termination of the P_n line around 5° for all profiles in Europe and the relatively short critical distances for the P_{m1} and P_{m2} branches has forced us to introduce an additional low-velocity zone between 45 and 60 km depth.

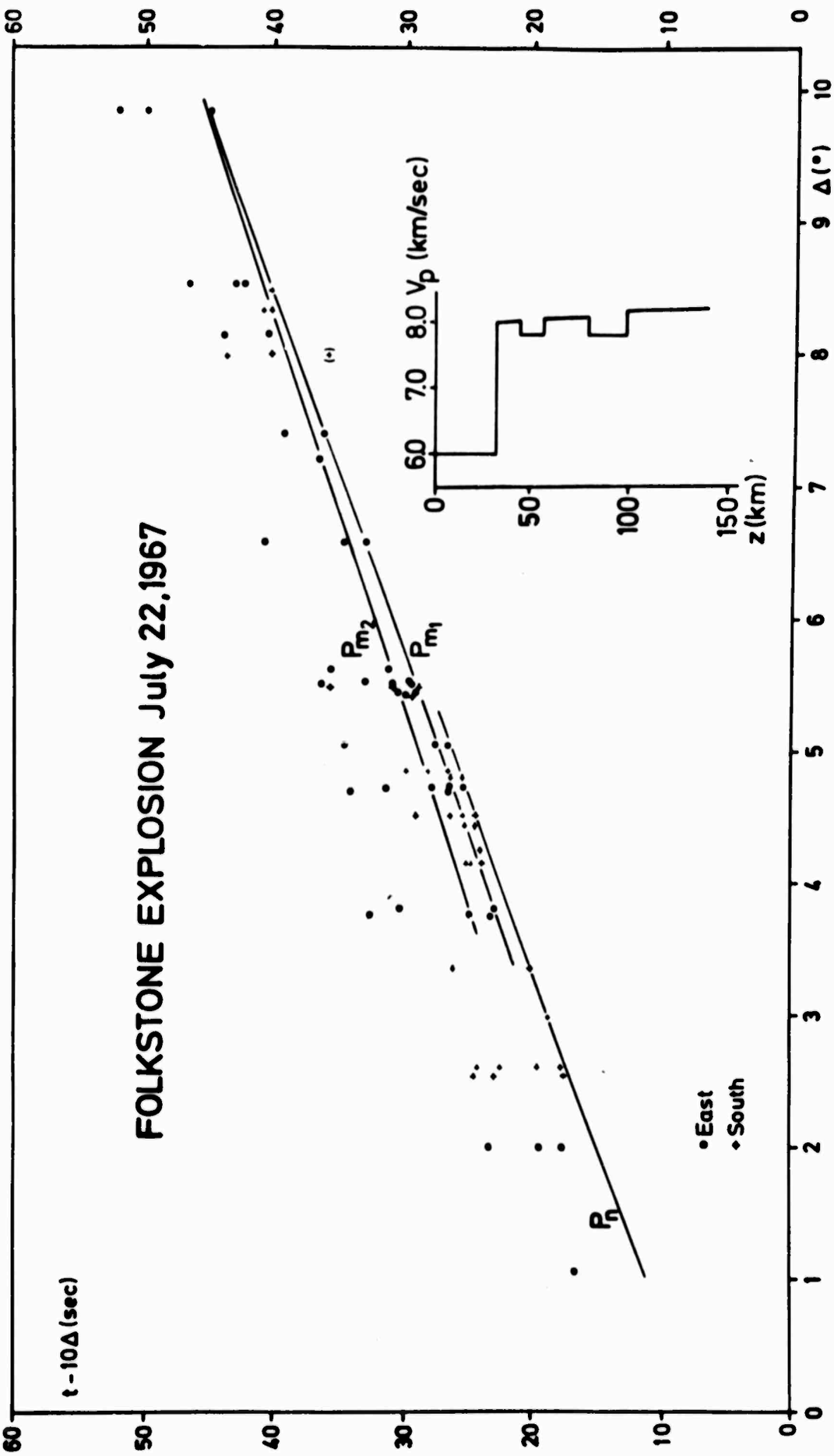

Fig. 16: Reduced travel times and velocity-depth structure for the FOLKSTONE Explosion of 22 July 1967

These results confirm the complexity of the uppermost mantle and indicate that at least three velocity reversals occur between the Mohorovičić discontinuity and the abrupt velocity increase postulated by LEHMANN (1959) at a depth of about 220 km, namely between

45	and	60	km,
80	and	100	km,
140	and	220	km.

4.12 Travel Times and Amplitude Spectra from Earthquakes (D. MAYER-ROSA)

At larger distances, i.e. for $5^{\circ} < \Delta < 30^{\circ}$, the travel-time data were supplemented by earthquake observations which, of course, lack the time resolution of the explosion measurements. In addition they are subject to the usual uncertainties in the epicenter and origin time determinations. A total of 600 events recorded at Stuttgart (STU) between 1937 and 1967 was chosen for this study. Epicentral distances were computed based on the focal data of the ISS up to 1961, and using the USCGS-Bulletin for the period 1961 through 1967. Accordingly the standard (root-mean-square) error of the travel-time determinations for P waves is $\pm$ 1.5 sec between 1937 and 1960, and $\pm$ 0.5 sec between 1961 and 1967. For S waves the error is about twice as high.

In Figs. 17 and 18 the measured P and S travel times are shown for two profiles directed SW and SE of Stuttgart, i. e. towards Spain and Greece. They were determined by observations of a multitude of events at a

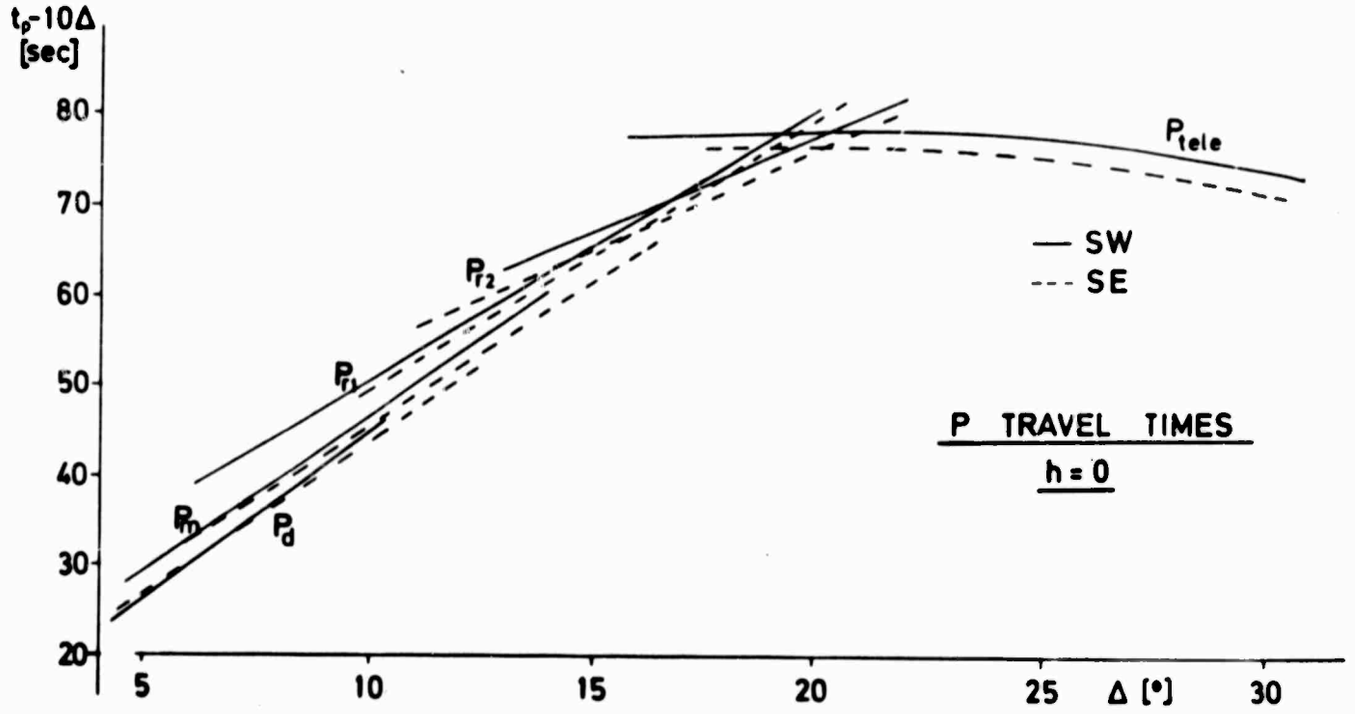

Fig. 17: P wave travel times from earthquakes (h=0)

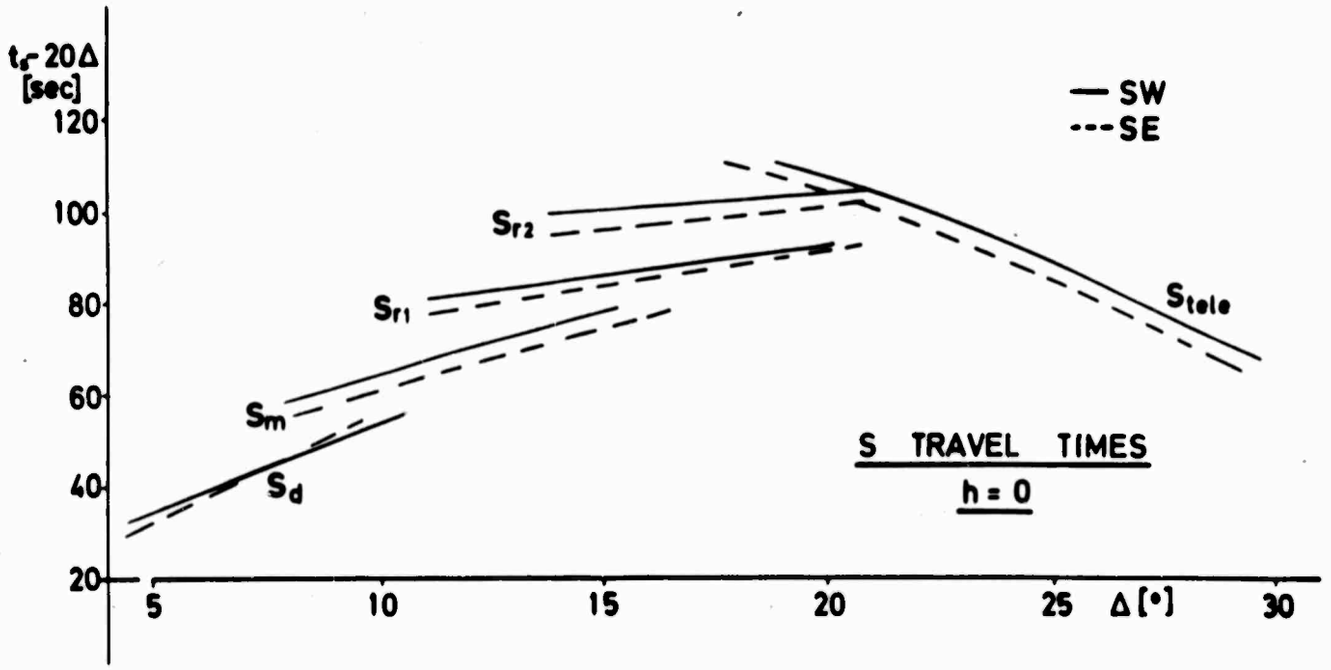

Fig. 18: S wave travel times from earthquakes (h=0)

fixed station (e.g. STU) and of selected events of suitable magnitude along a chosen array of European stations. An additional check was provided by the observed travel times of intermediate and deep focus earthquakes. All travel-time observations are corrected to zero focal depth and are reduced by 10Δ for P and 20Δ for S waves. In both cases five travel-time branches can be seen, namely

$P_d = P_n$	$S_d = S_n$
P_m	S_m
P_{r1}	S_{r1}
P_{r2}	S_{r2}
P_{tele}	S_{tele}

The apparent velocities of the first two branches are different for the SW and SE profiles, while the other three do not show any measurable differences in velocity. The SW travel-time curves, however, are consistently delayed by 2 sec in P, and by about 3 sec in S compared to the SE line. This immediately demonstrates that there must be pronounced regional differences in upper mantle structure. The considerable overlap of the various travel-time branches indicates that a much higher velocity contrast must exist at the corresponding depth, much higher than is suggested by the measured apparent velocities at the surface. Distinct velocity reversals for some depth intervals are therefore required to reconcile the results of theoretical computations with the observations.

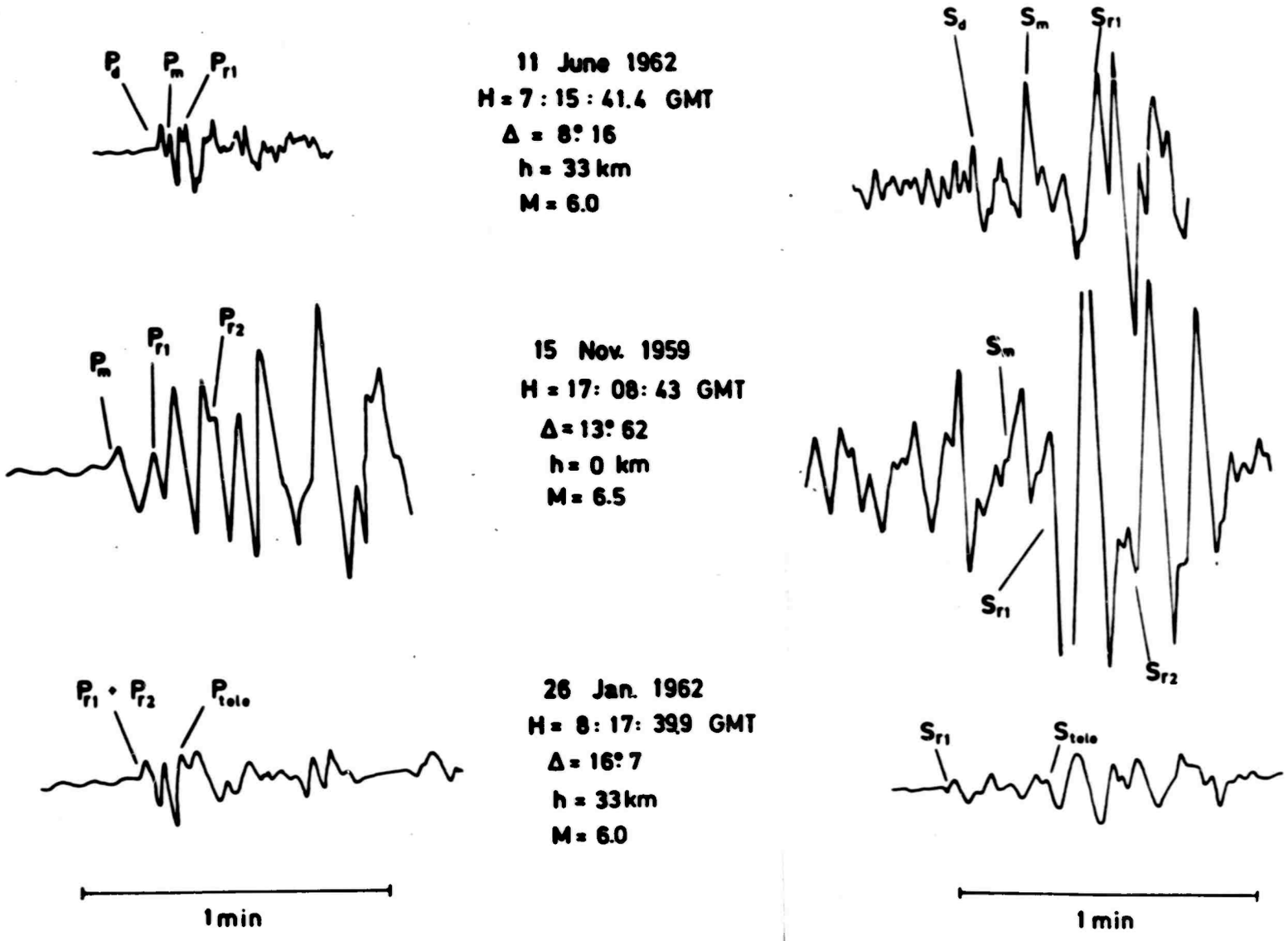

Fig. 19: Examples of mantle P and S phases

In Fig. 19 examples of the P and S wave groups are shown as recorded at distances of $8^{\circ}.2$, $13^{\circ}.6$ and $16^{\circ}.7$ (SE of Stuttgart). The magnitudes range from 6.0 to 6.5. As the recording instrument (Galitzin 12-12) and the "receiver crust" is the same in all cases, and if it is assumed that the "source crust" is about the same and that there is no directional effect of the source for the periods observed, then the spectral content of the various phases of the signal is solely determined by the propagation medium, i.e. by the path through the rather complex structure of the upper mantle.

The dominating periods (T) of P and S wave arrivals were determined as a function of distance by Fourier analysis and by visual analysis of the seismogram phases, as well as by spectrograph techniques (ref. EWING, MUELLER, LANDISMAN and SATÔ, 1959). The results are shown in Figs. 20 and 21. A more or less pronounced absorption effect can be seen for each of the different phases. Average Q values could be estimated from these data which are difficult to interpret in view of the complex velocity structure. The dominating periods increase systematically as the energy penetrates deeper and deeper into the mantle. Except for the teleseismic P and S branches the predominant periods in S are nearly twice as long as the values for P. From these periods and the corresponding wave lengths a lower limit for the thickness of the various layers through which the waves travel could be deduced.

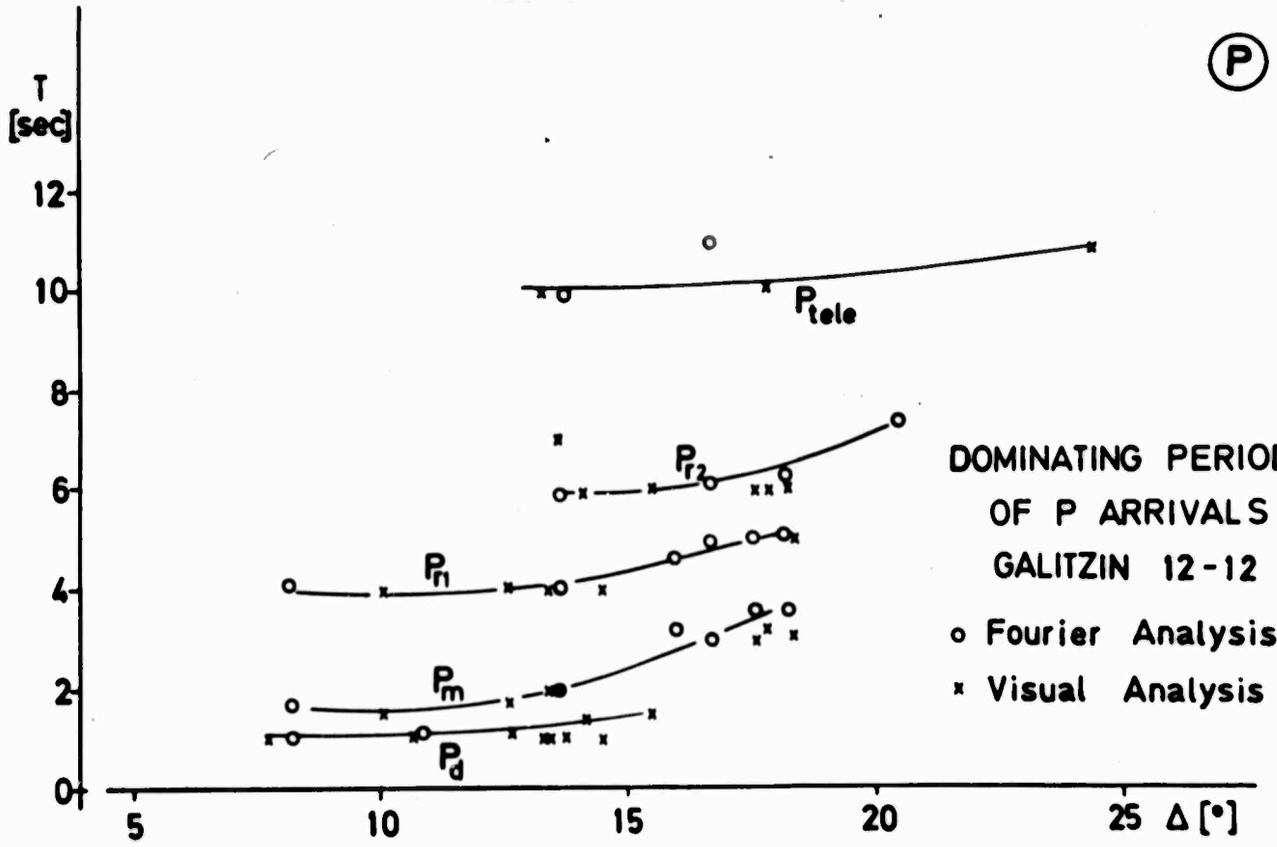

Fig. 20: Dominating wave periods of P arrivals

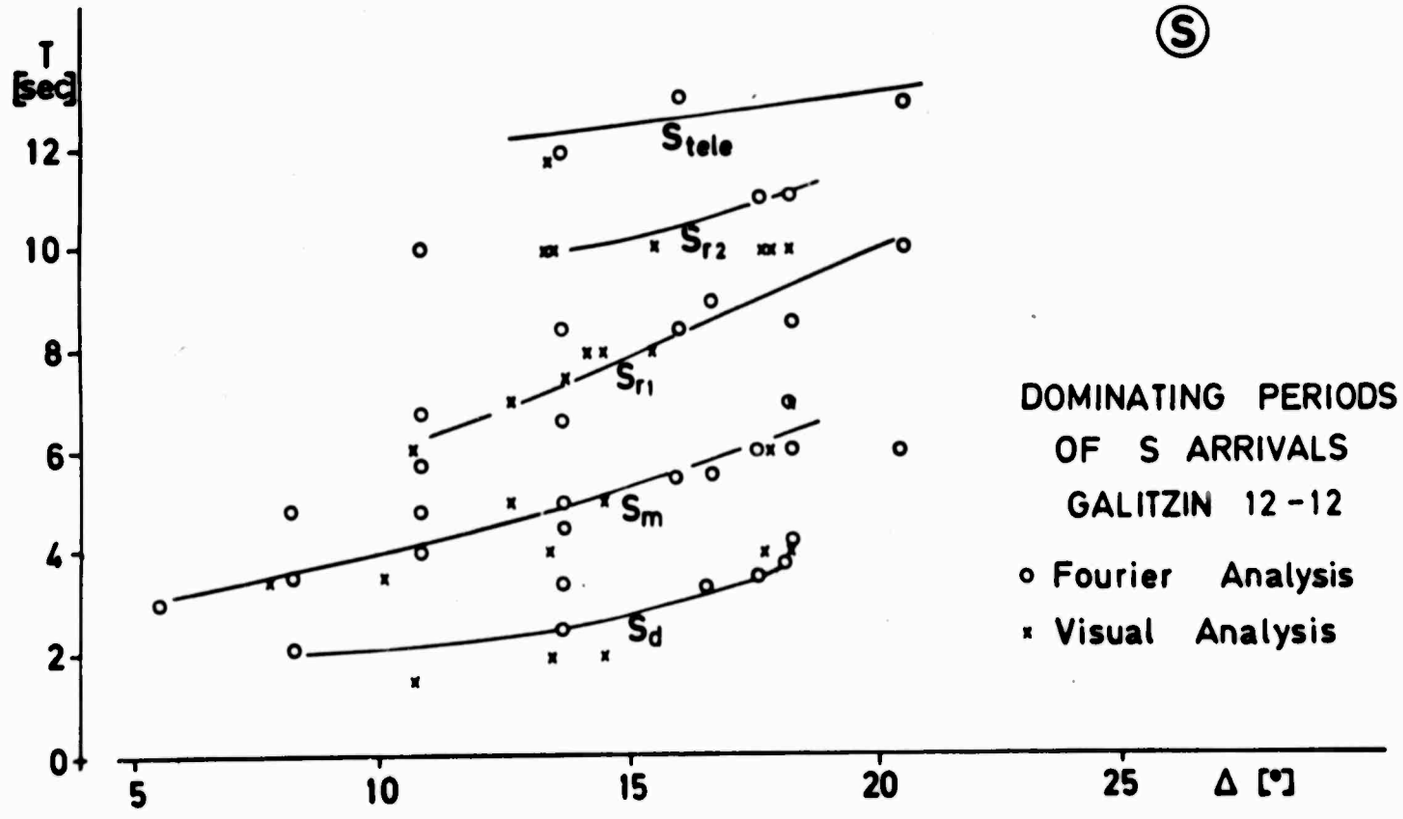

Fig. 21: Dominating wave periods of S arrivals

By trial and error velocity-depth distributions were derived which can explain the observed P and S travel times given in Figs. 17 and 18. They are depicted in Fig. 22. From the arguments presented above and similar conclusions arrived at by DOWLING and NUTTLI (1964) it was necessary to introduce a number of velocity reversals in order to explain the overlapping travel-time segments. Pronounced regional differences between the SW and SE profiles are noted down to depths of about 320 km. It should be pointed out specifically that a third low-velocity channel in S with a lower velocity contrast had to be assumed in the model calculations. The $S_{r1} - S_{r2}$ travel-time branches can only be explained by a velocity inversion between 260 and 320 km depth. For P waves the corresponding channel is either absent or so weak that it cannot be resolved with the present means of observation.

In Fig. 22 the velocity-depth profiles for Europe as proposed by LEHMANN (1959, 1961) are given for reference and comparison. It can be seen that the new P distribution oscillates around the old average value down to a depth of about 210-220 km. A similar "lamellar" structure of the upper mantle is found for S. The velocity inversions are much more severe than the single reversal which has been assumed to exist so far. If the lower channel boundaries are indeed as sharp as LEHMANN (1959, 1961) and others have suggested, then clear reflections should be observed. Evidence is found in the literature for North America (ref. KNOPOFF, MUELLER and PILANT, 1966) which confirms the postulate of LEHMANN (1962, 1964). In Europe we were able to trace at least parts

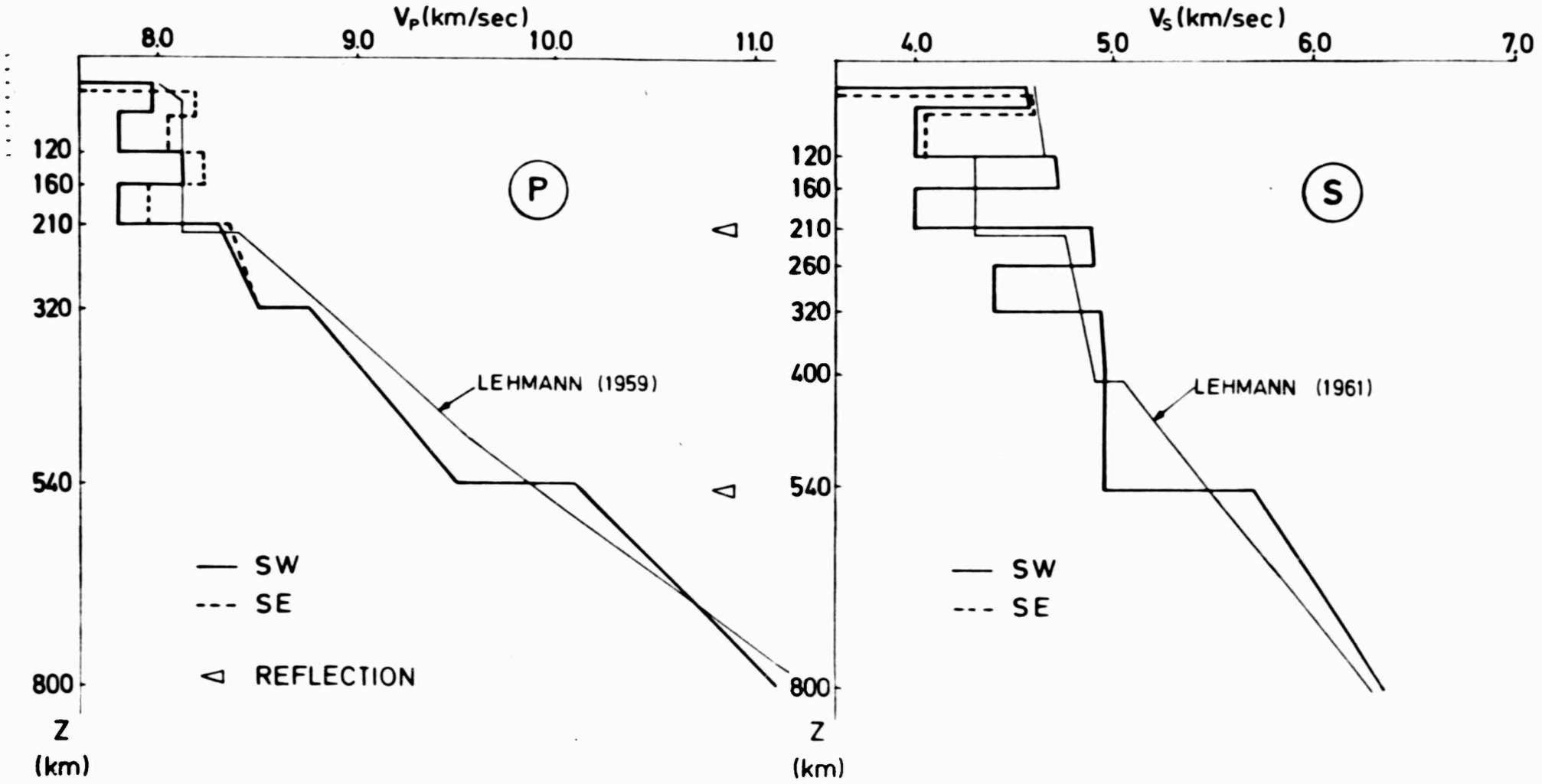

Fig. 22: New velocity-depht distributions for P and S waves

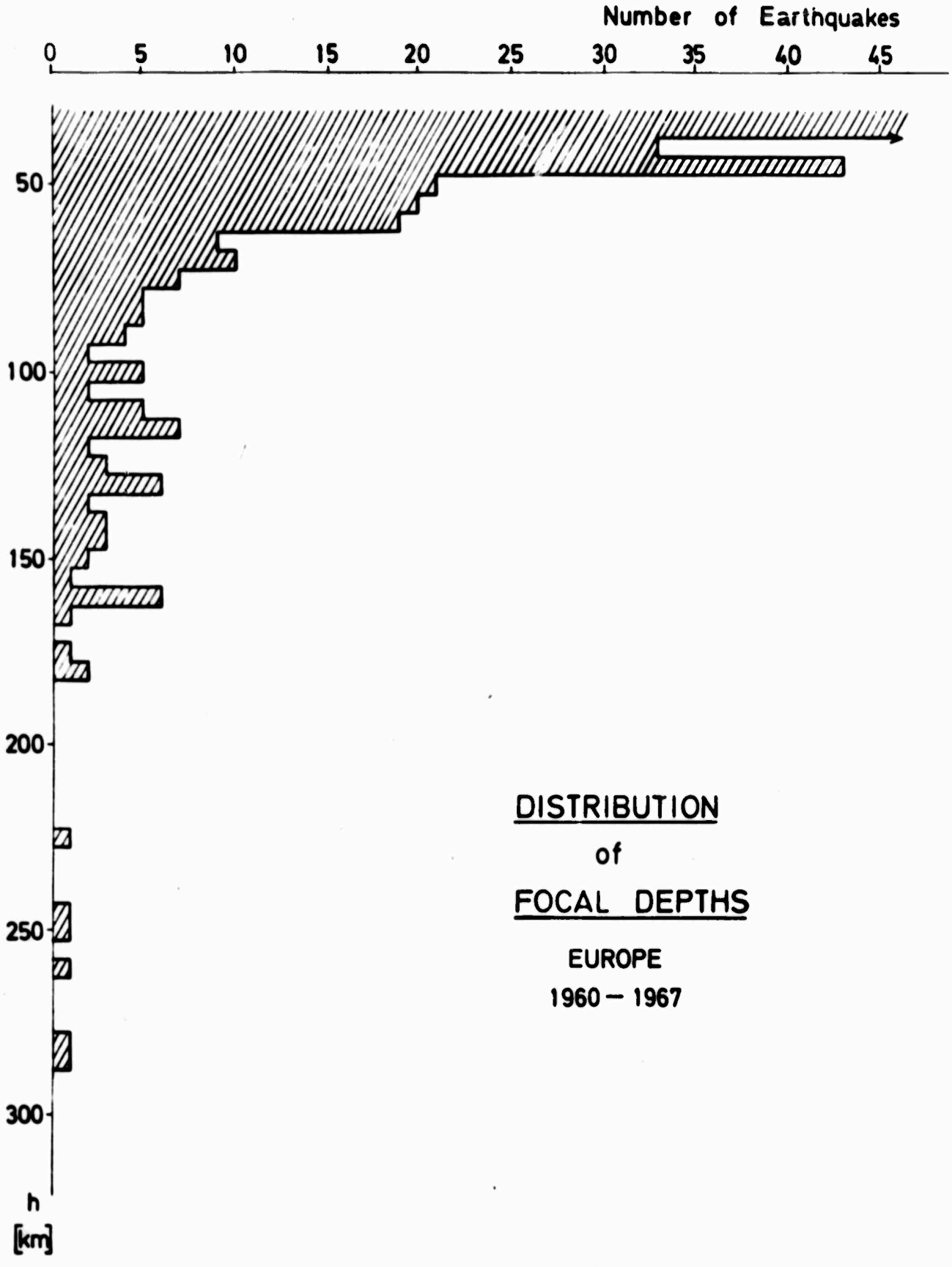

Fig. 23: Distribution of earthquake focal depths in Europe (1960 - 1967)

of two reflection hyperbolas which can be associated with pronounced discontinuities at depths of about 210 and 540 km.

Supporting evidence for the velocity-depth profiles presented in Fig. 22 comes from the distribution of earthquake focal depths in Europe. In Fig. 23 the number of earthquakes is plotted as a function of focal depth (h) for the time interval 1960-1967. These data are more reliable than the ones published previously for the European area. If the average depth ranges of the zones of velocity reversals are compared to the focal depth distribution it is found that they correlate well with the observed relative minima. In particular the concentration of foci close to the upper boundaries of the low-velocity channels as well as the complete absence of earthquakes with focal depths around 200 km should be noted. It is thus strongly emphasized that the structure of the upper mantle is much more complex than was implied by our previous models.

4.2 Dispersion of Seismic Surface Waves

(D. SEIDL)

Extensive studies of the dispersion characteristics of longer period surface waves of the Love and Rayleigh type have confirmed the existence of low-velocity layers in the upper mantle. They have also shown that there are pronounced regional variations in the velocity distribution with depth. The attenuation of long-period surface waves and the decay of the free oscillations of the earth depend in a very complicated way on the depth distribution

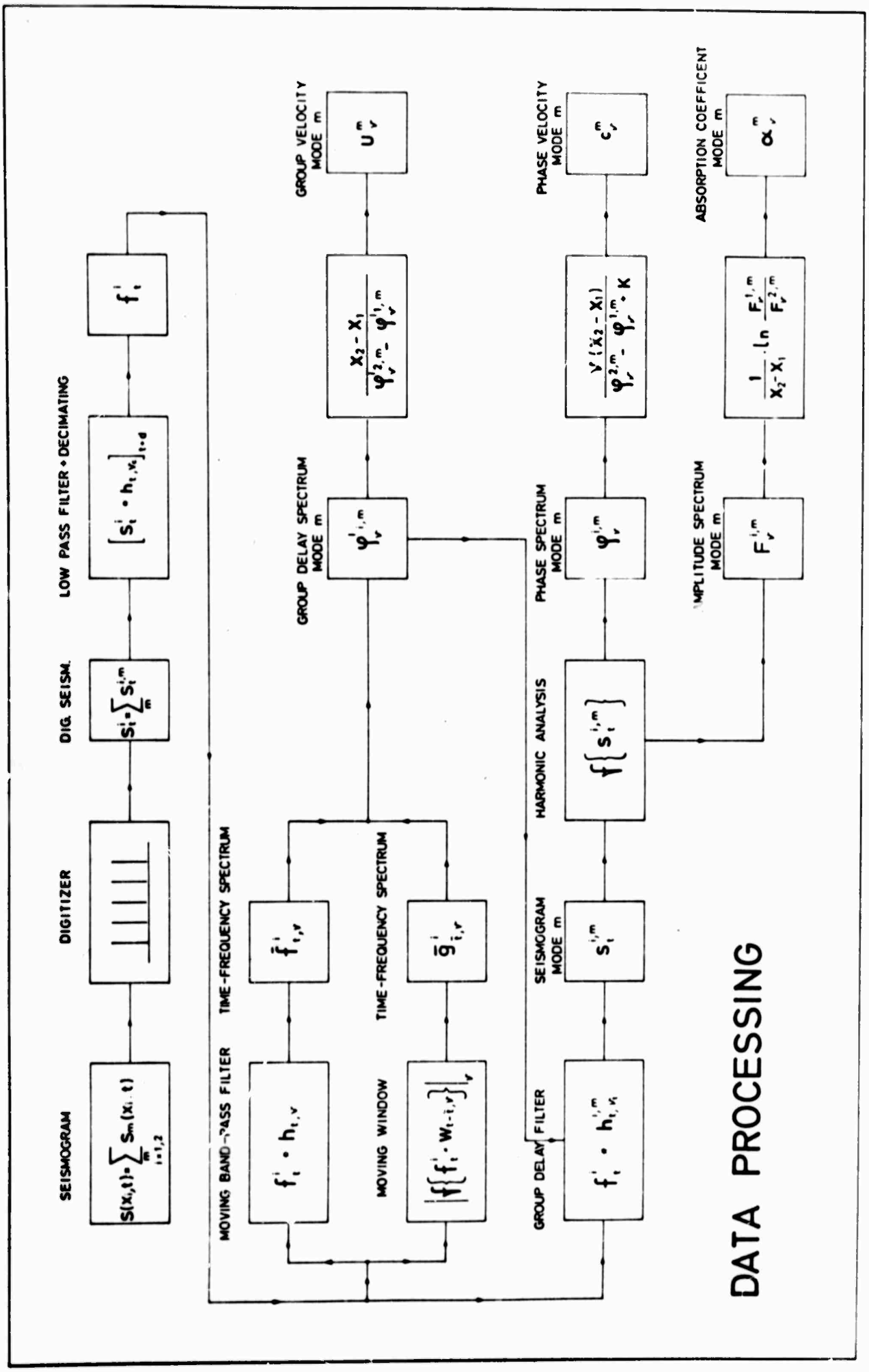

Fig. 24: Schematic block diagram of surface-wave data processing procedure

of parameters of elasticity and anelasticity. Complications caused by the source mechanism, instrumental distortion, path differences as well as low-velocity zones are, however, considerably reduced compared with body waves.

In Fig. 24 a block diagram of the data-processing procedure used in our surface wave studies is shown. Starting with a seismogram which can be thought of being a superposition of m normal (and leaking) modes the group and phase velocity dispersion as well as the absorption coefficient as a function of frequency (ν) can be determined for any two-station combination. Presently the data analysis is in progress for a trans-European profile from KEVO (Finland) to MALAGA (Spain).

During the past few years our attention has been focussed to the central European region and most recently to the Rhinegraben Rift-System (MUELLER, PETERSCHMITT, FUCHS and ANSORGE, 1967). The map in Fig. 25 summarizes the surface-wave observations in that area. Heavy lines indicate the station network used by SEIDL (1965) and SEIDL, MUELLER and KNOPOFF (1966) in their phase velocity measurements to the north of the Alps. Also shown by solid lines is the Alpine network of KNOPOFF, MUELLER and PILANT (1966). Tripartite results in the Alps produced evidence for a well-developed low-velocity channel for S with a shear velocity in the channel of 4.2 km/sec. Broken lines in Fig. 25 represent the new network around the Rhinegraben Rift- System which is nearly complete.

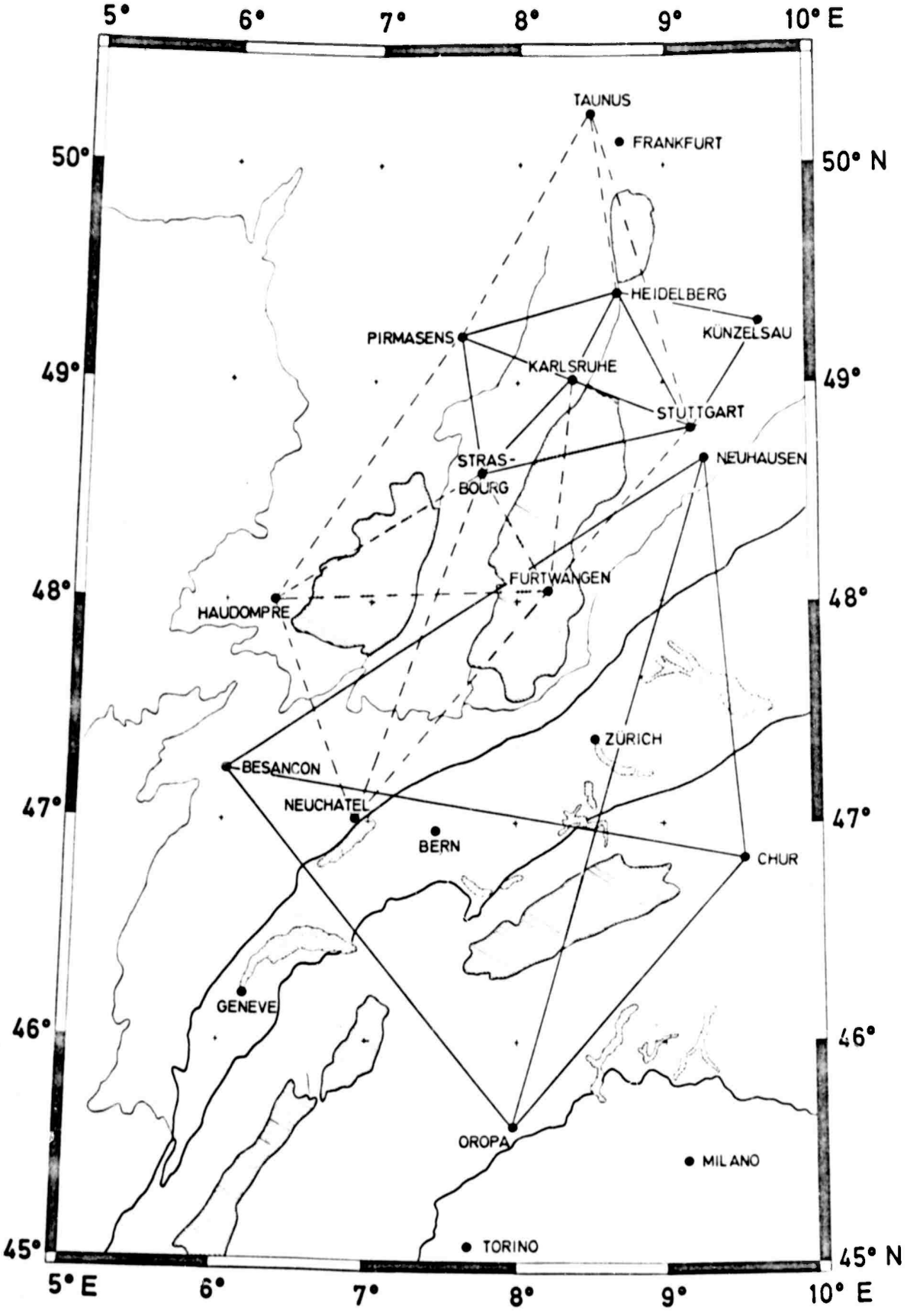

Fig. 25: Map of station network for dispersion measurements of surface waves

In our Annual Summary Report No. 1 (1966) a model of the crust and upper mantle has been reviewed which was termed STUTTGART (1) (ref. SCHNEIDER, MUELLER and KNOPOFF, 1966). It was primarily based on phase and group velocity measurements of Rayleigh waves for paths in the region of the Alps and through the foreland to the north. The rather scarce body-wave travel times available then were concordant with that model.

Based on additional studies of a number of near earthquakes (ref. SCHNEIDER, 1964) we have now deduced a new model which seems to be more representative for the average crustal and upper mantle structure in Central Europe. This new model, called STU-3 (see Table 3), consists of a four-layer crust in agreement with seismic refraction and near-earthquake observations. No efforts have been made so far to include the two low-velocity zones discussed above in this average c r u s t a l model. As before a sharp discontinuity is postulated at a depth of about 220 km which forms the lower boundary of the main asthenosphere low-velocity channel.

Observational data of fundamental mode Rayleigh waves for the lines Stuttgart-Strasbourg (SEIDL, MUELLER and KNOPOFF, 1966) and Stuttgart-Besançon (KNOPOFF, MUELLER and PILANT, 1966) which both traverse the Rhinegraben Rift System, are satisfactorily explained by model STU-3 (see Fig. 26). The phase-velocity results for the two Alpine lines Stuttgart-Oropa and Stuttgart-Chur are in better agreement with the old model STUTTGART 1 (ref. SCHNEIDER, MUELLER and KNOPOFF, 1966).

Depth (km)	Thickness (km)	V_P (km/s)	V_S (km/s)	Density (g/cm^3)
1.50	1.50	3.50	2.00	2.50
4.50	3.00	5.60	3.30	2.75
20.00	15.50	6.00	3.50	2.85
30.00	10.00	6.70	4.00	3.00
100.00	70.00	8.15	4.60	3.30
220.00	120.00	8.20	4.20	3.40
320.00	100.00	8.49	4.77	3.53
410.00	90.00	8.81	4.89	3.60
500.00	90.00	9.32	5.19	3.76
600.00	100.00	9.97	5.49	4.01
700.00	100.00	10.48	5.79	4.23
800.00	100.00	10.85	6.03	4.41
900.00	100.00	11.12	6.20	4.55
1000.00	100.00	11.33	6.32	4.64
1100.00	100.00	11.49	6.40	4.71
1200.00	100.00	11.64	6.47	4.77
1300.00	100.00	11.78	6.53	4.83
1400.00	100.00	11.92	6.59	4.88
1500.00	100.00	12.06	6.65	4.94
1600.00	100.00	12.19	6.70	5.00
1700.00	100.00	12.33	6.76	5.06
1800.00	100.00	12.46	6.81	5.11
1900.00	100.00	12.59	6.85	5.16
2000.00	100.00	12.72	6.90	5.21
2100.00	100.00	12.85	6.95	5.27
2200.00	100.00	12.97	7.00	5.32
2300.00	100.00	13.09	7.05	5.37
2400.00	100.00	13.21	7.10	5.42
2500.00	100.00	13.33	7.14	5.47
2600.00	100.00	13.46	7.19	5.52
2700.00	100.00	13.53	7.23	5.56
2800.00	100.00	13.61	7.28	5.61
		13.64	7.30	5.66

Table 3: Crust - Mantle Model STU - 3

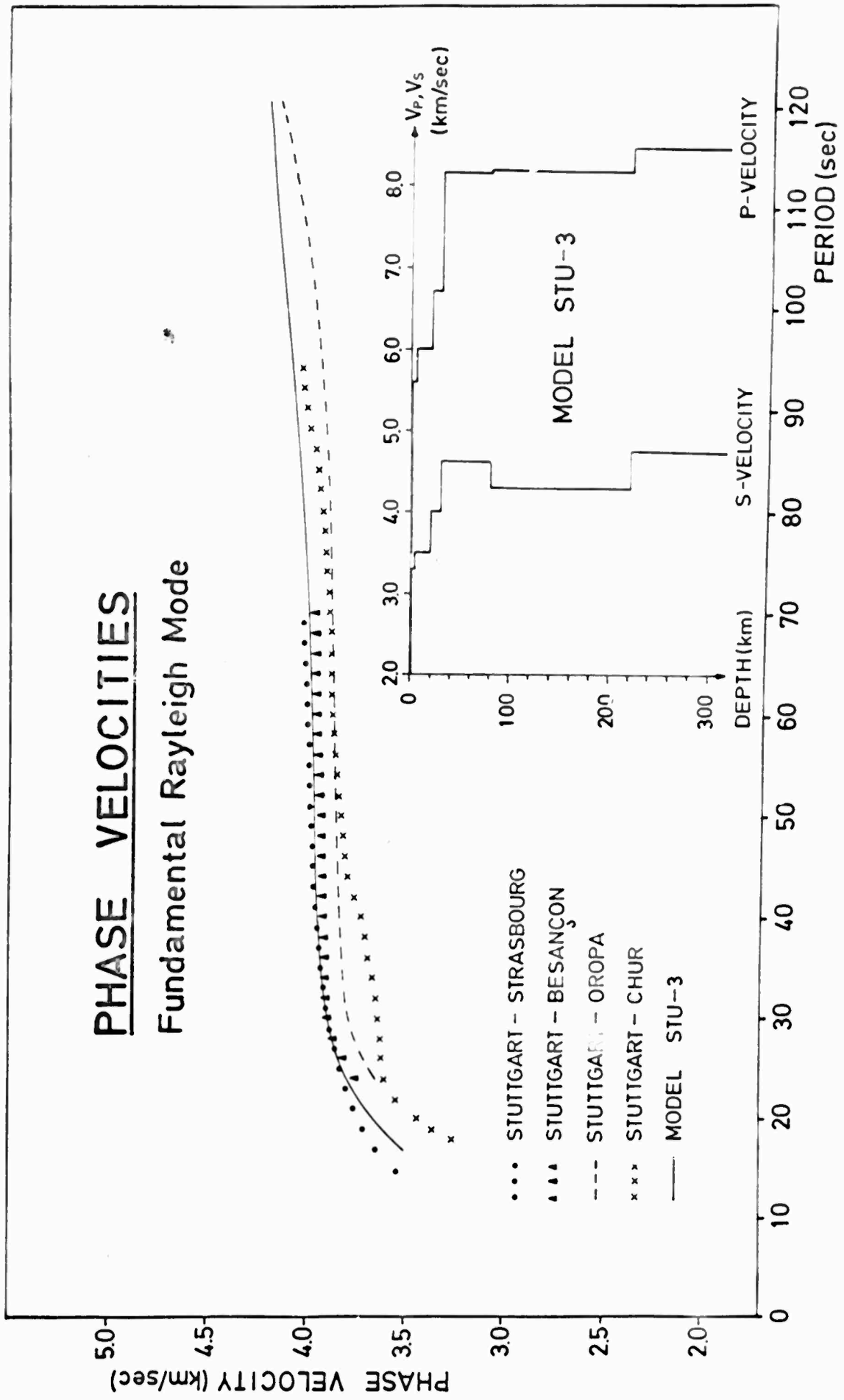

Fig. 26: Phase velocity measurements of Rayleigh waves in Central Europe and velocity-depth distribution for model STU-3

In contrast to this previously preferred structure the new model STU-3 contains only one layer above the channel in the upper mantle. The thickness of this lid (H_{LD}) has been increased by 20 km to 70 km, while the thickness of the channel (H_{CH}) has been decreased by the same amount to 120 km. All shear velocities above the channel are now slightly lower than before.

In Fig. 27 the partial derivatives of phase velocity are presented for model STU-3. The upper half of Fig. 27 shows how the phase velocity (c) of Rayleigh waves is altered by small variations of shear velocity in the channel (β_{CH}). In the lower half of Fig. 27 the changes of c caused by variations of the lid (H_{LD}) and channel (H_{CH}) thicknesses are displayed. It is seen that changes in the channel velocity (β_{CH}) are an order of magnitude more severe than variations in the geometrical configuration. If for the time being the complications indicated by body wave studies (see Fig. 22) are neglected, it is possible to explain all available dispersion data in Central Europe by slight modifications of model STU-3.

This simplified interpretation was justified until it became clear from body-wave results that there are at least two velocity reversals in the upper mantle, probably even three. In Fig. 28 (right) the phase velocity results for the line Stuttgart-Oropa are plotted as a function of wave period (T) or wave length (L), respectively. The latter quantity makes it easier to visualize the corresponding depth of

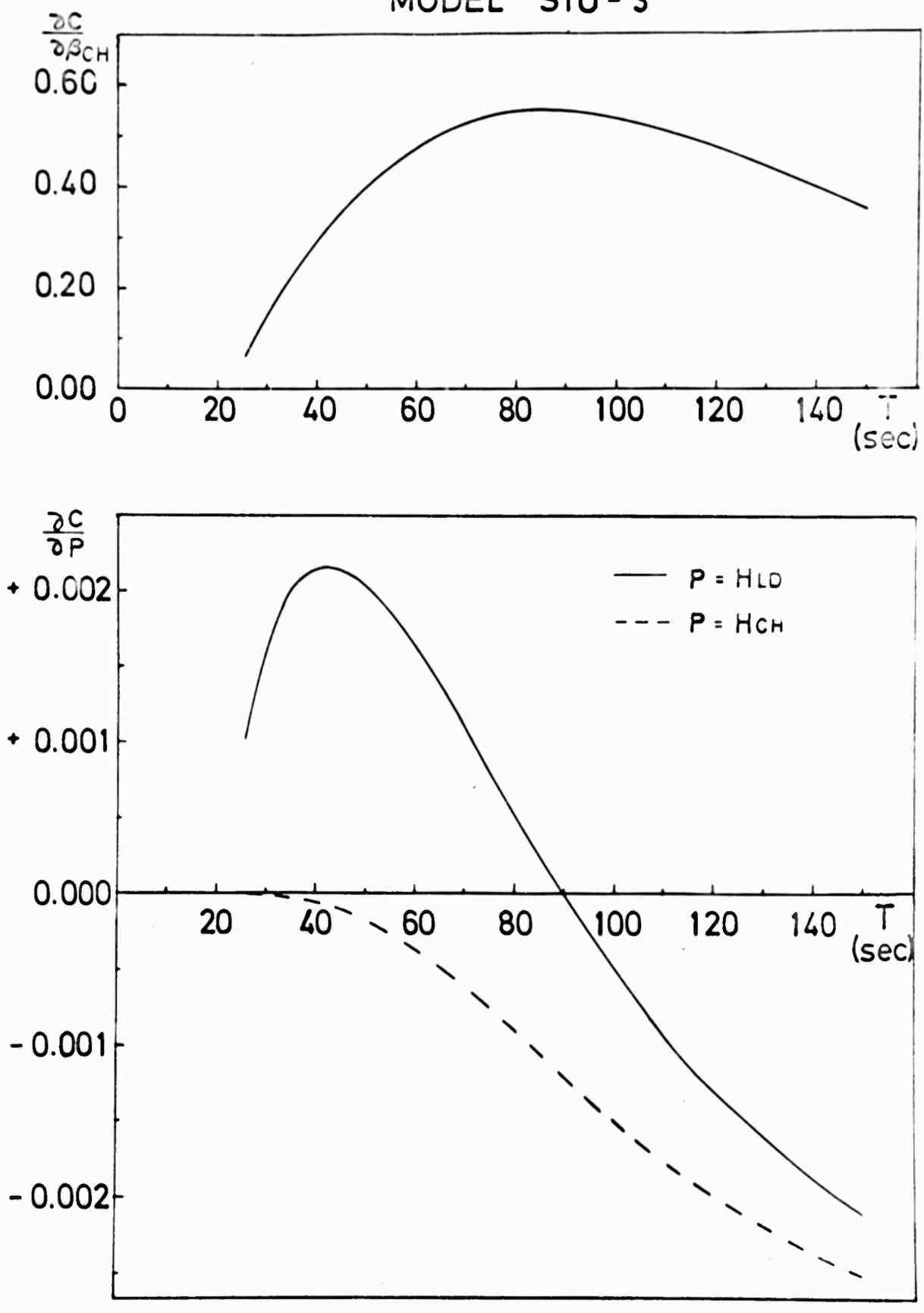

Fig. 27: Partial derivatives of phase velocity for model STU-3

penetration for these signals. Waves with the longest periods observed will "feel" the velocity distribution down to a depth of about 180 km. The fundamental mode and particularly the higher mode waves should therefore be sensitive to velocity inversions within the uppermost part of the mantle.

Phase velocities for two models which are based on the most recent travel-time analysis of explosion and earthquake data were calculated and are shown in Fig. 28. Model DARMSTADT 003 which evolved from Model (13) in Fig. 15 provides a satisfactory explanation of the dispersion measurements for the period range from 20 to 120 seconds. It should be kept in mind that the phase velocities for lines completely outside the Alps are on an average higher by about 0.10 to 0.15 km/sec, thus being in even better agreement with the theoretical results.

Model SW-Europe 160 uses the velocity distributions found from earthquake travel times (see Fig. 22). Except for the crustal structure which in the latter case has been adopted from investigations on the Iberian Peninsula (PAYO, 1965) there are pronounced differences in the number and depth intervals of the P and S velocity reversals. It is seen in Fig. 28 (right) that the calculated phase velocities are consistently too low in the intermediate period range. This is partly due to the different crustal structure assumed. The theoretical results should, therefore, not be compared to data from Central Europe. In addition the mean velocity of the uppermost 100 km seems to be too low. For all these reasons we presently prefer model DARMSTADT 003.

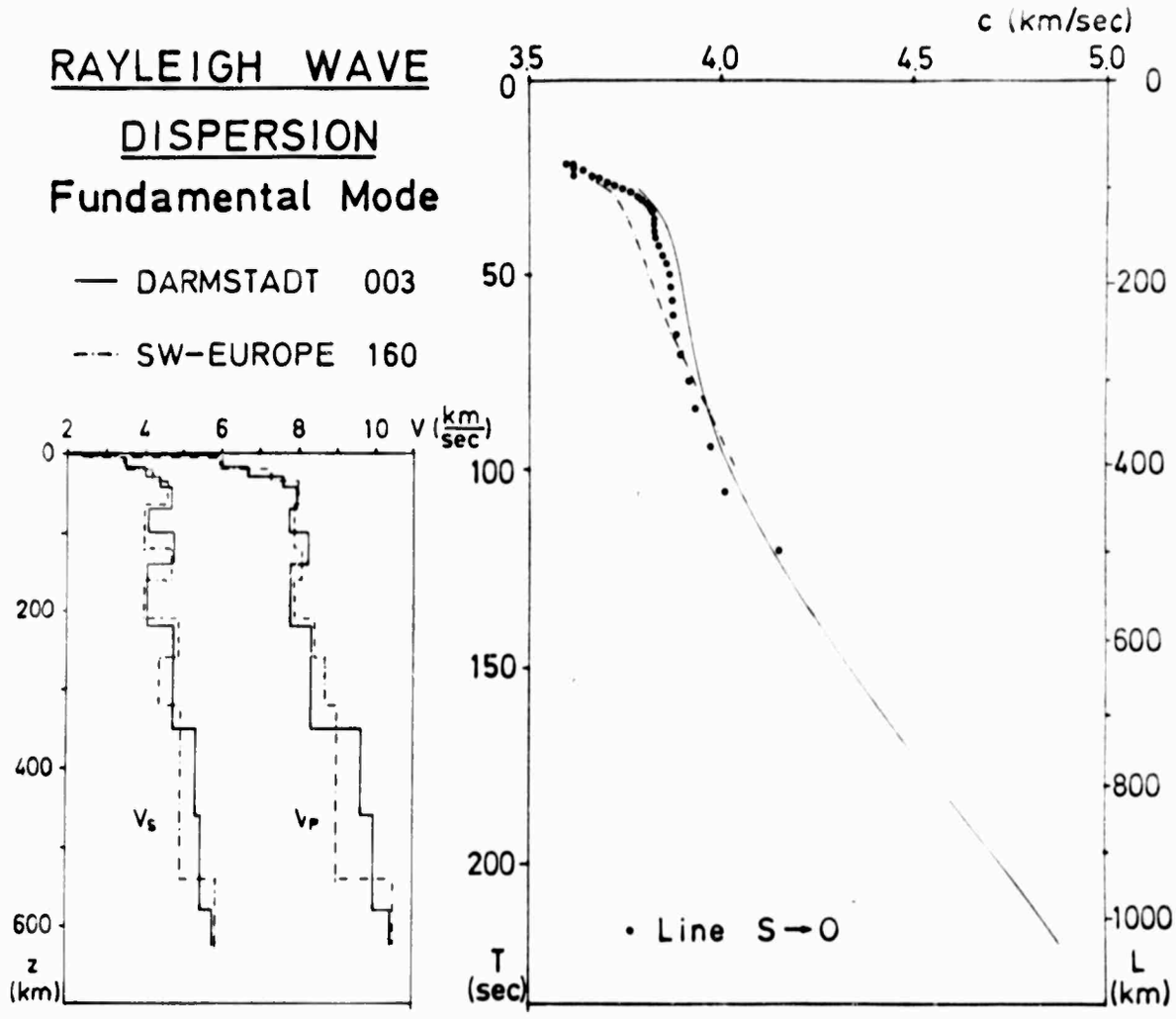

Fig. 28: Comparison of experimental Rayleigh wave dispersion results with theoretical calculations for the new models DARMSTADT 003 and SW-Europe 160

4.3 Amplitude Attenuation of Surface Waves

(U. WALTER)

Since amplitudes of body waves are particularly difficult to interpret because of source factors, mode conversion at interfaces, scattering, spreading losses and instrumental effects, a new technique has recently been developed for interpreting the frequency-dependent amplitude decay data of surface waves in terms of anelasticity versus depth (ANDERSON and ARCHAMBEAU, 1964; ANDERSON, BEN-MENAHEM and ARCHAMBEAU, 1965).

We Fourier-analyzed vertical pendulum records of several nuclear explosions in the atmosphere near Novaya Zemlya and also of a number of natural earthquakes in order to measure the phase and group velocities as well as the rate of decay of Rayleigh wave energy in the spectral band of about 10 to 100 seconds. These data are used to determine the attenuation in the upper mantle. In particular the eight events listed in Table 4 were studied:

(1) 23 October 1961
(2) 30 October 1961
(3) 5 August 1962
(4) 19 September 1962
(5) 25 September 1962
(6) 27 September 1962
(7) 22 October 1962
(8) 24 December 1962

Sample seismograms for the second event as recorded at Copenhagen (COP), Stuttgart (STU) and Strasbourg (STR) are reproduced in Fig. 29. Two interfering wave trains can be clearly discerned.

Table 4 : ATMOSPHERIC EXPLOSIONS NEAR NOVAYA ZEMLYA

(Origin times and epicentral coordinates by USCGS)

(1)	23 October	1961	08:31:22.1 GMT	73°.9 N	53°.8 E	M = 5.1	(UPP)
(2)	30 October	1961	08:33:27.8 GMT	73°.8 N	53°.5 E	M = 5.4	(UPP)
(3)	5 August	1962	09:08:45.8 GMT	74°.2 N	52°.5 E		
(4)	19 September	1962	11:00:56.4 GMT	73°.8 N	53°.8 E	M = 5-5.25	(PAL)
(5)	25 September	1962	13:02:31.7 GMT	73°.7 N	55°.0 E	M = 5.25	(PAL)
(6)	27 September	1962	08:03:16.4 GMT	74°.3 N	52°.4 E	M = 5.25-5.5	(PAL)
(7)	22 October	1962	09:06:10.1 GMT	73°.7 N	54°.2 E	M = 5-5.25	(PAL)
(8)	24 December	1962	11:11:42.0 GMT	73°.6 N	57°.5 E	M = 5.25	(KEW)

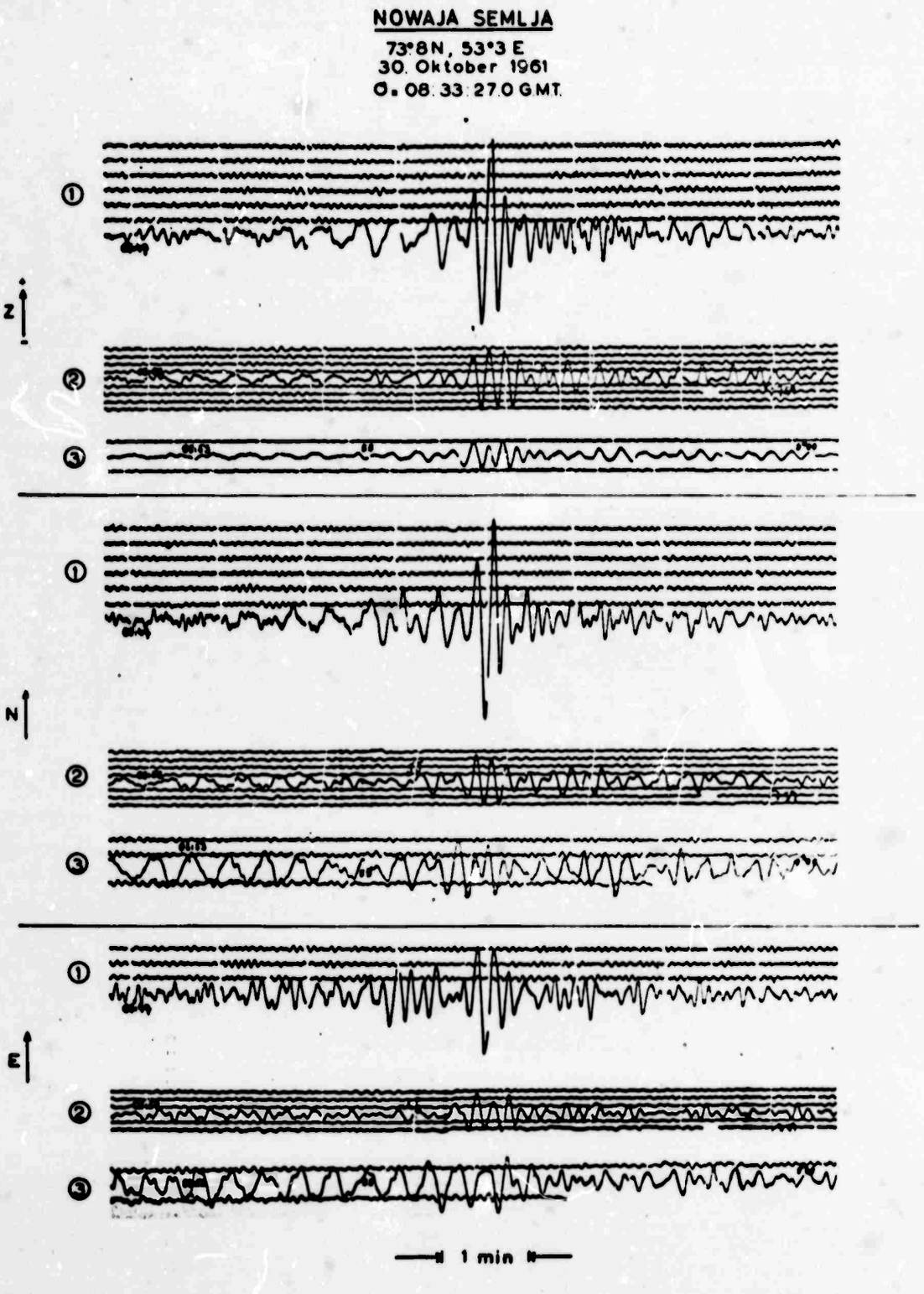

Fig. 29: Sample seismograms for the atmospheric explosion near Novaya Zemlya on 30 October 1961 as recorded at COP, STU and STR

Out of these eight explosions, the third and fourth were selected for a more extensive study. The long-period vertical records of the WWSS-Network for the available European stations were digitized over an interval covering the entire surface wave train. Reading inaccuracies could not be avoided in those parts of the seismogram where the amplitudes were largest. The digitized data were harmonically analyzed and the calculated Fourier amplitudes were then corrected for different peak magnification of the seismographs.

In Figs. 30 and 31 the computed amplitude spectra for selected stations are depicted. For reference the amplitude response of the 30-100 system then in operation at the WWSS stations is also shown. Fairly smooth spectra have been obtained for epicentral distances up to about 2 500 km, i.e. for stations located on the Fennoscandian shield. Severe deformations of the spectrum are observed as soon as the transition occurs between Fennoscandia and Central Europe. Changes in crustal structure must be responsible for the observed attenuation at the short-period end of the spectrum, while absorption in the uppermost mantle is the cause of the spectral degradation for periods greater than about 30 seconds.

Following TRYGGVASON (1965) an attempt has been made to determine the dimensionless quality factor Q for Rayleigh wave propagation across Europe. In the period range of around 40 to 50 seconds it has a value close to 250. A preliminary interpretation shows that Q must increase rapidly as the period decreases. At

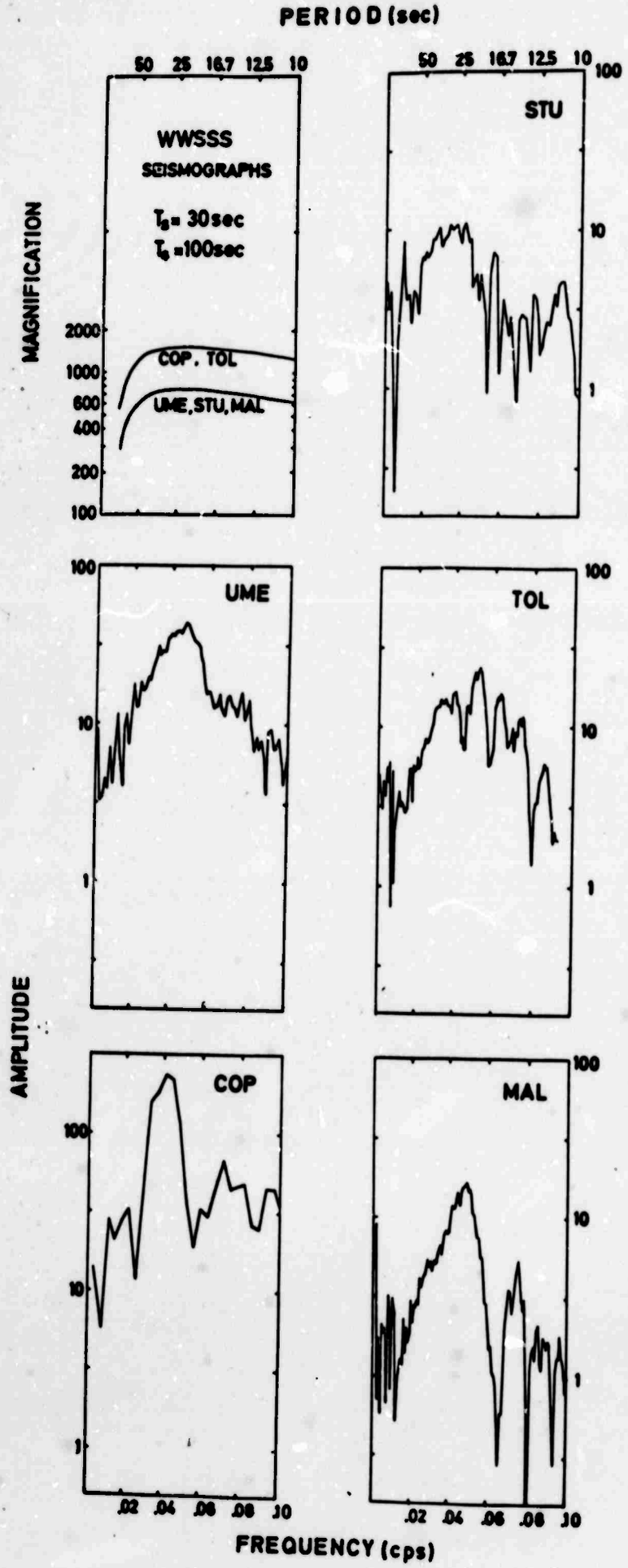

Fig. 30: Selected amplitude spectra of Rayleigh waves from the atmospheric explosion of 5 August 1962 near Novaya Zemlya. The response curves of the WWSS 30-100 seismographs are given for comparison

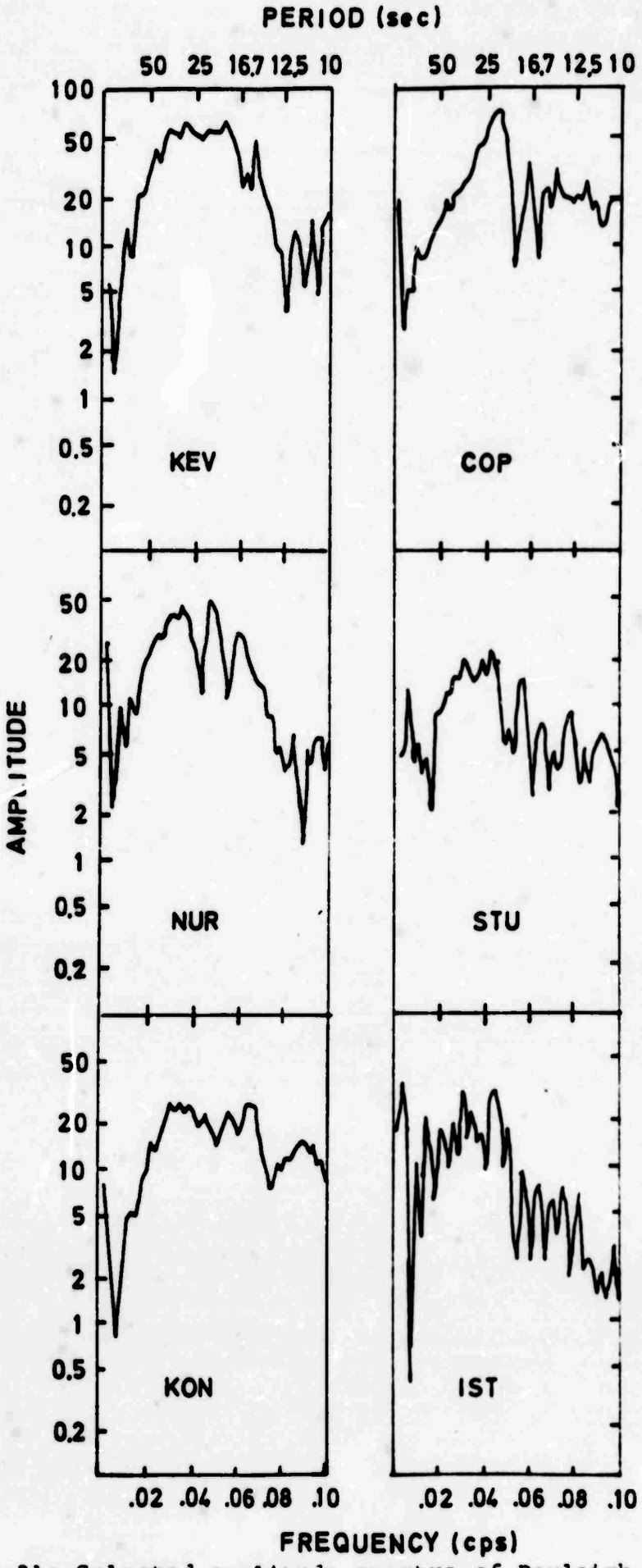

Fig. 31: Selected amplitude spectra of Rayleigh waves from the atmospheric explosion of 19 September 1962 near Novaya Zemlya

shorter periods and wave lengths corresponding to crustal dimensions the attenuation again increases, but the scatter of the data is too large and does therefore not permit any quantitative conclusions.

The amplitude decay data for Love (Q_L) and Rayleigh (Q_R) surface waves consistent with available body wave data are summarized in Fig. 32. Our Q_R average for Europe (o) is plotted together with TRYGGVASON's value (x) on top of the data points by ANDERSON, BEN-MENAHEM and ARCHAMBEAU (1965) for the paths Toledo-Trinidad and Chile-Pasadena. The specific quality factor Q is shown as a function of period (T). As before in Fig. 28 this type of display should make it easier to visualize the depth of penetration if the appropriate fractions of wave length are considered. Without too much imagination there is clear evidence for two zones of relatively low Q in the upper part of the mantle both for Love and Rayleigh waves, indicating that the increased attenuation is primarily due to losses in shear (Q_S).

A rough estimate shows that zones of low Q_S must exist at depths of about 80 - 110 km and 150 - 220 km. These depth intervals correspond to the depths found for the two main low-velocity channels discussed above. We conclude from these results that the simple Q model MM 8 proposed by ANDERSON, BEN-MENAHEM and ARCHAMBEAU (1965) is not adequate to explain the observations for periods smaller than 150 seconds. The Q values found for the crust

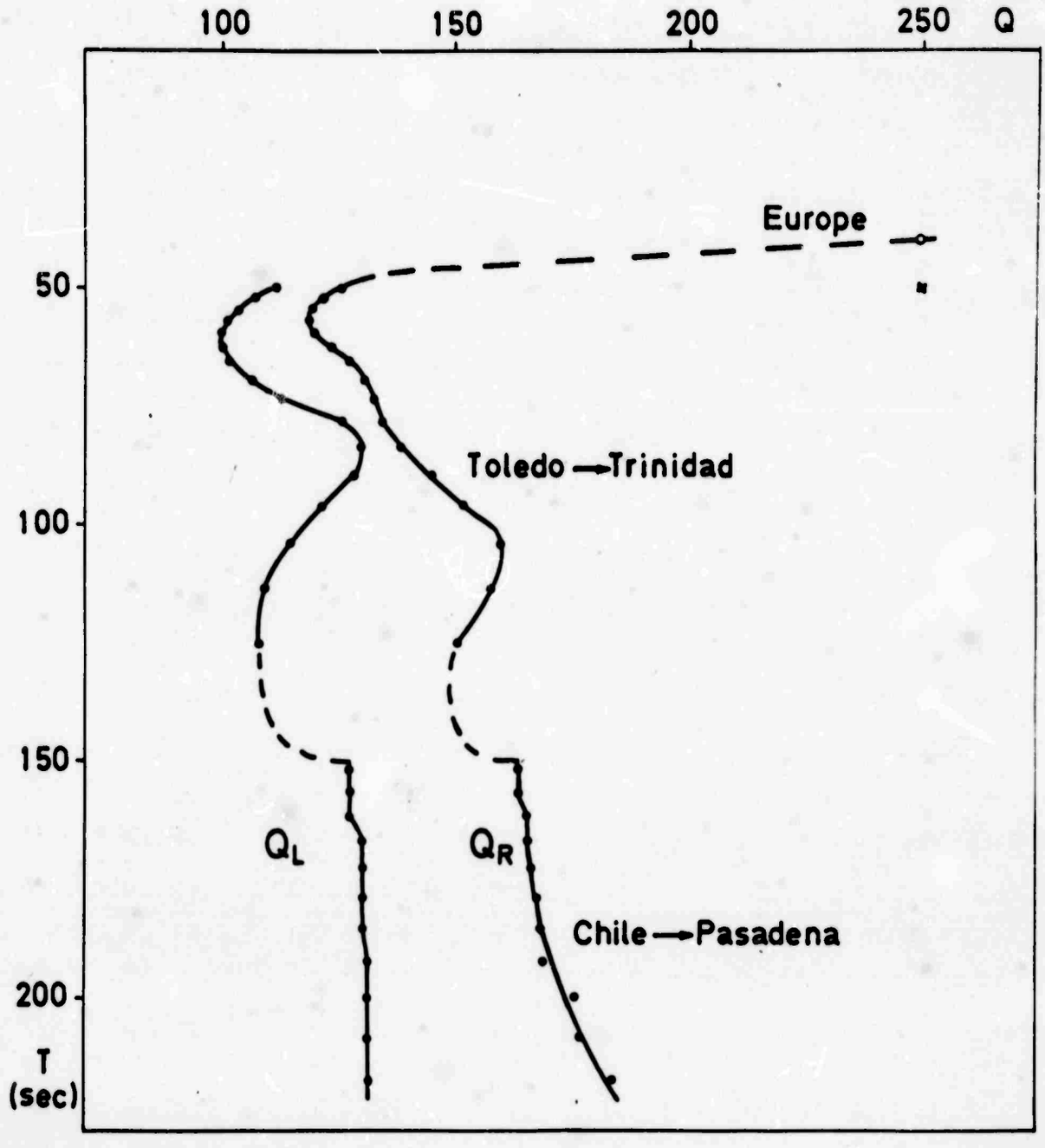

Fig. 32: Summary of attenuation data for Love (Q_L) and Rayleigh (Q_R) waves. The solid dots represent data by ANDERSON, BEN-MENAHEM and ARCHAMBEAU (1965), the x is a value by TRYGGVASON (1965), and o is our average value for Europe

are much lower than the ones deduced from the earlier results of PRESS (1964). Additional complications must be expected for the depth range immediately below the crust-mantle transition zone. Much more shorter-period data of improved quality are now needed to answer all these unsolved questions.

5. ANELASTIC PROPERTIES OF THE DEEPER MANTLE

5.1 Average Q of Compressional Waves ($\overline{Q_p}$)

(K.FUCHS)

A rough estimate of Q_p for the upper mantle has been obtained based on P observations of two Hindu Kush intermediate focus earthquakes (focal depth $h \approx 200$ km) as recorded at European and African WWSS network stations. The amplitude spectra of the P phases for the two shocks arranged according to increasing distance are displayed in Fig. 33. They have been corrected for instrumental distortion. Spectral corrections for the receiver crust have not yet been applied since not enough reliable information on crustal structure was available for all the stations. It is felt that the a v e r a g e $\overline{Q_p}$ which is determined from a number of stations with a wide variety of crustal structures should not be too much in error as the influence of the crust will cancel out to a first approximation.

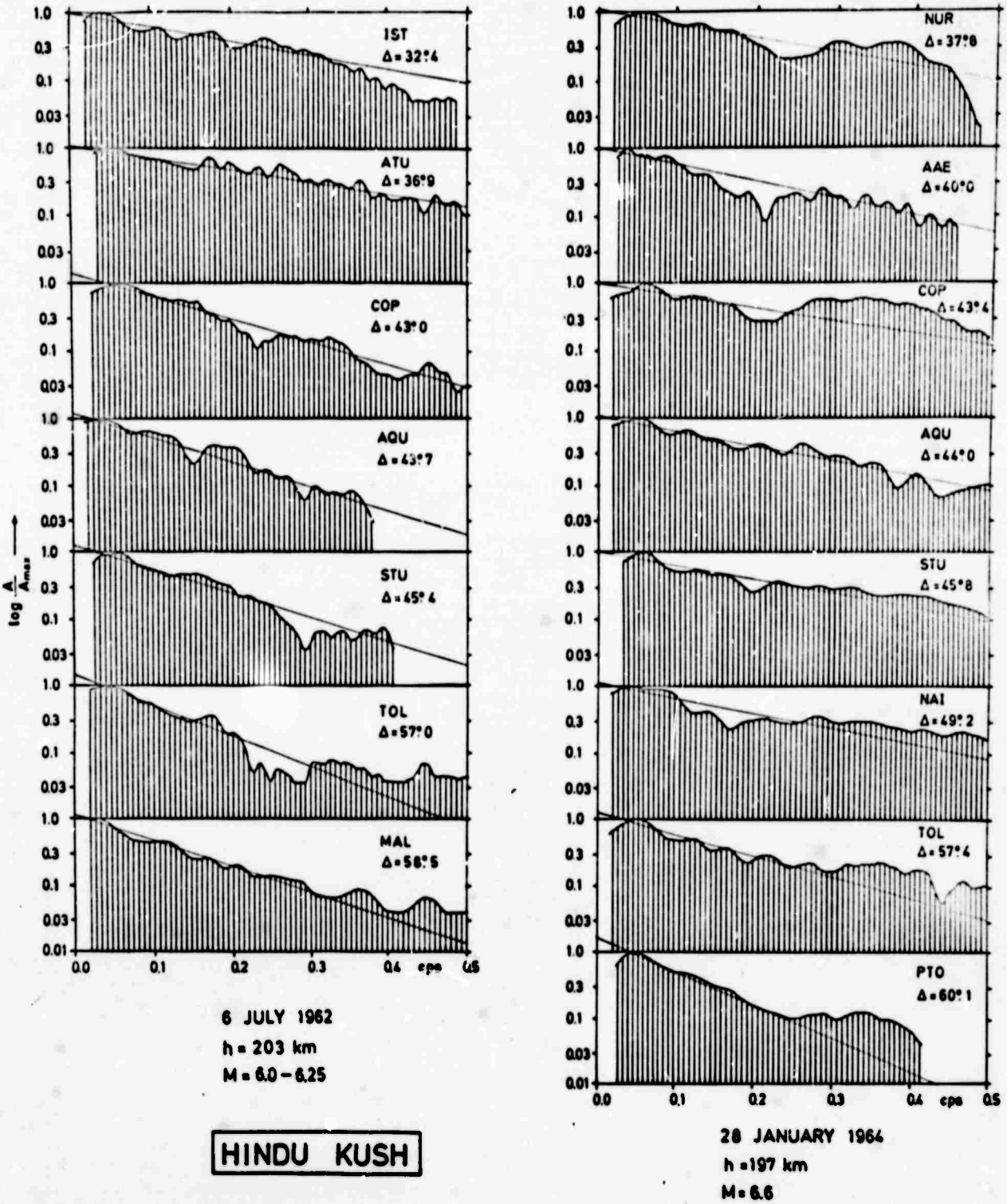

Fig. 33: Amplitude spectra of P waves from two Hindu Kush earthquakes of intermediate focal depth ($h \approx 200$ km)

If it is assumed that the intrinsic Q is independent of frequency as appears to be the case for most solid materials that have been measured in the laboratory, then the amplitude of a seismic phase may be expressed in the form:

$$A(\Delta, h, \omega) = \exp\left(-\frac{\omega}{2} \cdot \frac{t}{Q_p}\right)$$

In this equation t is the travel time along a ray starting at a deep focus of depth h and arriving at a station in the epicentral distance Δ.

Furthermore if it is assumed that the frequency-dependent amplitude distortion due to anelasticity is about the same for all rays above the depth of the focus, then the observed differences in spectral content must be attributed to those parts of the ray paths which have penetrated into the deeper mantle. More precisely only the propagation along rays through an earth model stripped down to the level of the focus ($h' \approx 200$ km) must be considered. To this end the stripped earth time t' for P observed at a station with epicentral distance Δ has been computed for different earth models using the same ray parameter p in the stripped earth which would correspond to the epicentral distance Δ and the focal depth h in the complete model.

With the above assumptions and $\omega = 2\pi\nu$ the amplitude spectrum can now be written as:

$$A(\nu) = \exp\left(-\frac{\pi t'}{Q_p}\nu + D(\nu)\right)$$

The term D (ν) takes care of the source spectrum which presumably is flat for all rays leaving the "focal window" within a narrow angle of aperture (8° in the present case). D (ν) also includes the effect of the ray segment above the stripped earth at the receiving end.

In Fig. 33 it is seen that the logarithms of the normalized amplitudes show a roughly linear dependence on frequency ν within the observed spectral range. Therefore to a first approximation D (ν) must also be linearly dependent on frequency within that range:

$$D(\nu) = - E \cdot \nu$$

The measured spectral gradients $B = \ln A/\nu$ and the corresponding stripped earth times t' of a Jeffreys-Bullen earth model were then used to determine a r.m.s. best-fit line to the equation:

$$B = \frac{\pi}{\overline{Q_p}} t' + E$$

For the two events the results are as follows:

6 July 1962: $\overline{Q_p} = 149 \pm 40$, $E = 1.6 \pm 2.4$

28 Jan. 1964: $\overline{Q_p} = 201 \pm 86$, $E = 1.5 \pm 3.0$

With the high error limits the assumption $E = 0$ seems to be justified, i.e. the source spectrum must be essentially flat within the frequency range considered. Again fitting a r.m.s. line to the data results in:

6 July 1962: $\overline{Q_p} = 179 \pm 5$

28 Jan. 1964: $\overline{Q_p} = 256 \pm 11$

It follows that the average Q_p value ($Q_p \approx 220$) for the deeper part of the mantle, i.e. for depths between 200 and 1600 km is much lower than the values which have been reported in the literature so far.

5.2 Implications on Loss Mechanisms

A complete description of possible loss mechanisms in the earth requires the measurement of the attenuation of compressional and shear waves. According to KOVACH and ANDERSON (1964) an average value of 200 for $\overline{Q_S}$ in the upper 600 km of the mantle satifies the observational data. The average $\overline{Q_S}$ of 600 in the whole mantle and the value for $\overline{Q_S}$ of 200 in the upper mantle leads to an estimate of 2200 for the average $\overline{Q_S}$ of the lower mantle. This number is an order of magnitude greater than the Q_S in the upper mantle. The observed distribution of Q_S with depth suggested by these body wave results seemed to agree with the Q_S distribution inferred from torsional oscillation data and Love wave observations of ANDERSON and ARCHAMBEAU (1964).

A promising approach in determining the attenuation of compressional waves in the mantle has been suggested by KOVACH (1967). The logarithm of the spectral amplitude ratio of SKP and SKS permits the attenuation of compressional waves (Q_p) in the mantle to be compared to that of shear waves (Q_S) since the effects of the source and of the common propagation paths can be eliminated. Preliminary

results indicate that the average $\overline{Q_p}$ for the whole mantle is about 500, i.e. comparable to the average $\overline{Q_s}$ of 600 in the mantle and much lower than has been assumed until recently.

Several years ago CARPENTER and FLINN (1965) presented results which seemed to indicate that the following proportionality holds:

$$\overline{Q_p} = k \cdot t_p$$

It was claimed that this relation with $1.00 < k < 1.25$ holds for P signals recorded at teleseismic distances ($\Delta > 20^\circ$) from s h a l l o w events. Attenuating effects of both the source and the receiver system are thus included in the analysis. The data presented in this report suggest that except for the crustal segment of the ray paths the average $\overline{Q_p}$ is only about one half of the mean value obtained from the above proportionality relation. This is at least substantiated by our P observations in the period range $2 < T < 20$ sec and for epicentral distances out to 60°, i.e. down to depths of about 1500-1600 km.

A recent study by TENG (1968) has again led to the generally accepted result that the lower mantle has a much higher Q than the upper mantle. But the rapid increase of Q_p postulated now must occur at a depth of about 950 to 1000 km, considerably deeper than the estimates of 450 km (ANDERSON, BEN-MENAHEM and ARCHAMBEAU, 1965) and 650 km (KNOPOFF, 1964). By assuming no losses in pure compression

Q_p should be approximately 2.5 times Q_S, thus ruling out major nonadiabatic or thermal conduction losses. Under this assumption ANDERSON, BEN-MENAHEM and ARCHAMBEAU (1965) have derived a Q_p model for the mantle from their Q_S structure that is obtained by inverting surface-wave data.

In agreement with TENG (1968) we find that our results are closer to $Q_p \approx Q_S$, and that consequently losses in pure compression are not negligible. Similar conclusions have also been reached by KANAMORI (1967 a+b) for periods of 1-2 seconds. Even if allowance is made for experimental uncertainties, the discrepancy between the body-wave and surface-wave results seems to be significant. It is thus indicated that $\overline{Q_S}$ around 1-2 sec period may be smaller by a factor of 2 compared to $\overline{Q_S}$ around 25-50 sec period, i.e. that $\overline{Q_S}$ decreases with increasing frequency.

These results would suggest that the approximation of a frequency-independent Q does not hold over a wider frequency band. A frequency dependence of Q cannot be established at this point because of the paucity of data. But if the result $Q_p \approx Q_S$ is accepted, losses in pure compression are no longer small or negligible compared to losses in shear, and loss mechanisms such as for example thermoelasticity cannot be ruled out completely.

6. REFERENCES

ANDERSON, D.L. and R.L. KOVACH, Attenuation in the mantle and rigidity of the core from multiply reflected core phases, Proc. Natl.Acad.Sci.U.S., 51, 168-172, 1964.

ANDERSON, D.L. and C.B. ARCHAMBEAU, The anelasticity of the earth, Journ.Geophys.Res., 69, 2071-2084, 1964.

ANDERSON, D.L., A. BEN-MENAHEM and C.B. ARCHAMBEAU, Attenuation of seismic energy in the upper mantle, Journ.Geophys.Res., 70, 1441-1448, 1965.

BEAUFILS, Y., P. MECHLER et Y. ROCARD, Résultats du tir du Lac de l'Eychauda, Ann.Géophys., 21, 287-291, 1965.

BEN-MENAHEM, A., S. SMITH and T. TENG, A procedure for source studies from spectrums of long-period seismic body waves, Bull.Seism.Soc. Amer., 55, 203-236, 1965.

BEN-MENAHEM, A., Observed attenuation and Q values of seismic surface waves in the upper mantle, Journ.Geophys.Res., 70, 4641-4651, 1965.

CARPENTER, E.W. and E.A. FLINN, Attenuation of teleseismic body waves, Nature, 207, 745-746, 1965.

DEMENITSKAYA, R.M., Basic features of the earth's crust structure on geophysical data, Trans.Sci.Res.Inst.of Arctic Geology, 115, 222p., 1961.

DOWLING, J. and O. NUTTLI, Travel time curves for a low velocity channel in the upper mantle, Bull.Seism.Soc.Amer., 54, 1981-1996, 1964.

EWING, M., St. MUELLER, M. LANDISMAN and Y. SATO, Transient analysis of earthquake and explosion arrivals, Geofisica Pura e Applicata, 44, 83-118, 1959.

FERNANDEZ, L.M., Master curves for the response of layered systems to compressional seismic waves, Bull.Seism.Soc.Amer., 57, 515-543, 1967.

FUCHS, K., The transfer function for P-waves for a system consisting of a point source in a layered medium, Bull.Seism.Soc.Amer., 56, 75-108, 1966.

FUCHS, K. and M. LANDISMAN, Result of a re-interpretation of the N-S-refraction line Adelebsen-Hildersheim in Western Germany, Ztschr.f.Geophysik, 32, 121-123, 1966a.

FUCHS, K. and M. LANDISMAN, Detailed crustal investigation along a north-south-section through the central part of Western Germany, Amer.Geophys.Union Geophys.Monograph, 10, 433-452, 1966b.

GERMAN RESEARCH GROUP FOR EXPLOSION SEISMOLOGY, Crustal structure in Western Germany, Ztschr.f. Geophysik, 30, 209-234, 1964.

HANNON, W.J., An application of the HASKELL-THOMSON matrix method to the synthesis of surface motion due to dilatational waves, Bull.Seism. Soc.Amer., 54, 2067-2079, 1964.

HIRSCHLEBER, H., J. HJELME and M. SELLEVOLL, A refraction profile through the northern Jutland, Geodaetisk Institut Meddelelse No. 41, Copenhagen, 34p., 1966.

KANAMORI, H., Spectrum of P and PcP in relation to the mantle-core boundary and attenuation in the mantle, Journ.Geophys.Res., 72, 559-571, 1967a.

KANAMORI, H., Spectrum of short-period core phases in relation to the attenuation in the mantle, Journ.Geophys.Res., 72, 2181-2186, 1967b.

KNOPOFF, L., "Q", Rev.Geophys., 2, 625-660, 1964.

KNOPOFF, L., St. MUELLER and W.L. PILANT, Structure of the crust and upper mantle in the Alps from the phase velocity of Rayleigh waves, Bull.Seism.Soc.Amer., 56, 1009-1044, 1966.

KOVACH, R.L. and D.L. ANDERSON, Attenuation of shear waves in the upper and lower mantle. Bull. Seism.Soc.Amer., 54, 1855-1864, 1964.

KOVACH, R.L., Attenuation of seismic body waves in the mantle, Geophys.Journ.R.A.S., 14, 165-170, 1967.

LANDISMAN, M. and St. MUELLER, Seismic studies of the earth's crust in continents; Part II: Analysis of wave propagation in continents and adjacent shelf areas, Geophys.Journ. R.A.S., 10, 539-554, 1966.

LANDISMAN, M., St. MUELLER and K. FUCHS, Further evidence for the sialic low-velocity zone in continental areas, Geophys.Journ.R.A.S., 13, 367-368, 1967.

LEHMANN, I., Velocities of longitudinal waves in the upper part of the earth's mantle, Ann.Géophys., 15, 93-118, 1959.

LEHMANN, I., S and the structure of the upper mantle, Geophys.Journ.R.A.S., 4, 124-138, 1961.

LEHMANN, I., The travel times of the longitudinal waves of the Logan and Blanca atomic explosions and their velocities in the upper mantle, Bull.Seism.Soc.Amer., 52, 519-526, 1962.

LEHMANN, I., On the travel times of P as determined from nuclear explosions, Bull.Seism.Soc. Amer., 54, 123-139, 1964.

LITVINENKO, I.V. and K.A. NEKRASOVA, Observations of deep seismic sounding in the Baltic Shield, Collection of paper on deep seismic sounding of the earth's crust in the USSR, 187-206, Gostoptebehizdat, Leningrad.

MUELLER, St. and M. LANDISMAN, Seismic studies of the earth's crust in continents; Part I: Evidence for a low-velocity zone in the upper part of the lithosphere, Geophys. Journ.R.A.S., 10, 525-538, 1966.

MUELLER, St. and K. FUCHS, Investigations on the nonelastic behavior of the upper mantle, Annual Summary Report No. 1, AFOSR Contr. AF 61 (052)-861, 52p., 1966.

MUELLER, St., E. PETERSCHMITT, K. FUCHS and J. ANSORGE, The rift structure of the crust and upper mantle beneath the Rhinegraben, Abh.Geol. Landesamt Baden-Württemberg, 6, 108-113, 1967.

MUELLER, St., J. ANSORGE, D. MAYER-ROSA and K. FUCHS, Evidence for several velocity reversals in the upper mantle, Ztschr.f.Geophysik, 34 (in press), 1968.

O'BRIEN, P.N.S., Quantitative discussion on seismic amplitudes produced by explosions in Lake Superior, Journ.Geophys.Res., 72, 2569-2575, 1967.

PAYO, G., Iberian peninsula crustal structure from surface wave dispersion, Bull.Seism.Soc. Amer., 55, 727-743, 1965.

PENTTILÄ, E., On seismological investigation of crustal structure of Finland, Publ.No.60, Inst.of Seismology, University of Helsinki, 1965.

PHINNEY, R.A., Structure of the earth's crust from spectral behavior of long-period body waves, Journ.Geophys.Res., 69, 2997-3017, 1964.

PRESS, F., Seismic wave attenuation in the crust, Journ.Geophys.Res., 69, 4417-4418, 1964.

SCHNEIDER, G., Die Erdbeben in Baden-Württemberg 1955-1962, Veröffentlichung d. Landeserdbebendienstes Baden-Württemberg, Stuttgart, 46p., 1964.

SCHNEIDER, G., St. MUELLER and L. KNOPOFF, Gruppengeschwindigkeitsmessungen an kurzperiodischen Oberflächenwellen in Mitteleuropa, Ztschr.f.Geophysik, 32, 33-57, 1966.

SEIDL, D., Die Struktur der Erdkruste und des oberen Erdmantels in Südwestdeutschland nach Phasengeschwindigkeitsmessungen an Rayleigh-Wellen, Thesis, Technische Hochschule, Stuttgart, 79p., 1965.

SEIDL, D., St. MUELLER and L. KNOPOFF, Dispersion von Rayleigh-Wellen in Südwestdeutschland und in den Alpen, Ztschr.f.Geophysik, 32, 472-481, 1966.

TENG, T.L., Attenuation of body waves and the Q structure of the mantle, Journ.Geophys. Res., 73, 2195-2208, 1968.

TRYGGVASON, E., Dissipation of Rayleigh wave energy, Journ.Geophys.Res., 70, 1449-1455, 1965.

7. CHRONOLOGICAL BIBLIOGRAPHY

The following reports on work performed during the duration of this contract have been completed and delivered to the European Office of Aerospace Research (EOAR):

Type of Report		Period Covered
Letter Planning Report (Administrative Report)	No. 1	1 May 1965 - 31 May 1965
Quarterly Narrative Progress Report (Scientific Report)	No. 1	1 May 1965 - 31 July 1965
" "	No. 2	1 Aug. 1965 - 31 Oct. 1965
" "	No. 3	1 Nov. 1965 - 31 Jan. 1966
Annual Summary Report	No. 1	1 May 1965 - 30 April 1966
Quarterly Narrative Progress Report (Scientific Report)	No. 4	1 May 1966 - 31 July 1966
" "	No. 5	1 Aug. 1966 - 31 Oct. 1966
" "	No. 6	1 Nov. 1966 - 31 Jan. 1967
Progress Report	No. 7	1 Febr. 1967 - 30 April 1967
" "	No. 8	1 May 1967 - 31 July 1967
" "	No. 9	1 Aug. 1967 - 31 Oct. 1967
Final Scientific Report		1 May 1965 - 30 April 1968

These reports were supplemented by

Special Scientific Report No. 1, dated 20 May 1966 , on
" Seismic Ground Noise and Wind at the Seismological Observatory Graefenberg "
by H. BERCKHEMER and B. AKASCHE .

As a result of this contract work a number of publications will soon be available. The first paper has just been published:

DOHR, G. and K. FUCHS, Statistical evaluation of deep crustal reflections in Western Germany, Geophysics, 32, 951-967, 1967

Three papers are about to be published:

FUCHS, K., Das Reflexions- und Transmissionsvermögen eines geschichteten Mediums bei beliebiger Tiefenverteilung der elastischen Moduln und der Dichte für schrägen Einfall ebener Wellen, Ztschr.f.Geophysik, 34 (in press), 1968

MUELLER, St., J. ANSORGE, D. MAYER-ROSA and K. FUCHS, Evidence for several velocity reversals in the upper mantle, Ztschr.f.Geophysik, 34 (in press), 1968

FUCHS, K., On the properties of deep crustal reflectors, Ztschr.f.Geophysik, 34 (in press), 1968

Four more papers with the following titles are in preparation:

(1) " Structure of the crust and uppermost mantle in the eastern part of France "

(2) " Das Durchlaßspektrum der Erdkruste in Europa für langperiodische seismische Raumwellen "

(3) " Energieverluste seismischer Raumwellen in der Erdkruste und im obersten Erdmantel "

(4) " Attenuation of compressional waves in the earth's mantle "

Security Classification UNCLASSIFIED

DOCUMENT CONTROL DATA - R&D

(Security classification of title, body of abstract and indexing annotation must be entered when the overall report is classified)

1. ORIGINATING ACTIVITY (Corporate author)
Geophysical Institute
Technical University
Karlsruhe, Germany

2a. REPORT SECURITY CLASSIFICATION
Unclassified

2b. GROUP

3. REPORT TITLE

INVESTIGATIONS ON THE NONELASTIC BEHAVIOR OF THE UPPER MANTLE

4. DESCRIPTIVE NOTES (Type of report and inclusive dates)
SCIENTIFIC FINAL 1 May 1965 - 30 April 1968

5. AUTHOR(S) (Last name, first name, initial)

M U E L L E R , Stephan

6. REPORT DATE	7a. TOTAL NO. OF PAGES	7b. NO. OF REFS
20 May 1968	71	45

8a. CONTRACT OR GRANT NO.	9a. ORIGINATOR'S REPORT NUMBER(S)
AF 61 (052)-861	
b. PROJECT AND TASK NO. 9714-612	
c. DOD ELEMENT 6250601 R	9b. OTHER REPORT NO(S) (Any other numbers that may be assigned this report) AFOSR 68-1932
d. DOD SUBELEMENT	

10. DISTRIBUTION STATEMENT
This document has been approved for public release and sale; its distribution is unlimited

11. SUPPLEMENTARY NOTES
Tech, Other

12. SPONSORING MILITARY ACTIVITY
AF Office of Scientific Research (SRPG)
1400 Wilson Boulevard
Arlington, Virginia 22209

13. ABSTRACT

The attenuation of seismic waves in the crust and upper mantle has been studied by various techniques in order to determine the specific quality factor Q. Anelastic deficiencies of the propagation medium can only be separated after corrections are made for the effects of instrumental distortion, of the "receiver crust" and the "source crust", the lossless propagation through the mantle and the source mechanism.

Seismic refraction data have been compiled for a number of "source" and "receiver" regions in Europe. A refined velocity-depth distribution with two velocity reversals and an average value of $Q_P \approx 670$ have been obtained for the crust of the Bohemian Massif in Central Europe. The Q_P of the uppermost mantle was found to be about 250. Crustal transfer functions were calculated to test models of crustal structure derived by other methods. The radiation patterns for two types of explosive sources have been determined. Their shape is strongly affected by the source mechanism and crustal structure.

A new velocity-depth structure of the upper mantle in Europe has been derived from travel-time observations of large explosions and earthquakes. At least three velocity reversals have been found down to depths of about 220 km. They correlate well with the distribution of earthquake focal depths. Surface-wave dispersion measurements are also in agreement with these new findings. Amplitude decay data for surface waves indicate that zones of low Q_S must exist at depths where the low-velocity channels were found.

DD FORM 1 JAN 64 1473

UNCLASSIFIED

Security Classification

13. Abstract (continued)

Finally an average value of $\overline{Q_p} \approx 220$ for the deeper mantle has been obtained based on observations of two intermediate focus earthquakes. A comparison with corresponding $\overline{Q_S}$ data shows that $Q_p \approx Q_S$, i.e. that losses in pure compression cannot be neglected. Alternatively it is suggested that Q may be frequency-dependent, at least over an extended frequency band.

14. KEY WORDS	LINK A		LINK B		LINK C	
	ROLE	WT	ROLE	WT	ROLE	WT
Amplitude Decay						
Amplitude Spectra						
Anelastic Properties						
Asthenosphere Channel						
Attenuation						
Crustal Structure						
Crustal Transfer Function						
Crust-Mantle System						
Deep Reflections						
Dispersion of Surface Waves						
Earthquake Focal Depths						
Electrical Conductivity						
High-Velocity (Intermediate) Layer						
Instrumental Distortion						
Linear System Theory						
Loss Mechanisms						
Low-Velocity Zones						
Nonelastic Behavior						
Phase Velocity of Surface Waves						
Q (= Specific Quality Factor)						
Radiation Pattern of Source						
Receiver Crust (System)						
Seismic Refraction						
Seismic Wave Propagation						
Source Crust (System)						
Source Mechanisms						
Specific Quality Factor (= Q)						
Spectral Analysis						
Spectral Behavior of Crust and Mantle						
Travel Times of Body Waves						
Upper Mantle Structure						
Velocity-Depth Distribution						
Velocity Gradients						
Velocity Reversals						